
Surface-ocean dynamics during eccentricity minima: a comparison between interglacial Marine Isotope Stage (MIS) 1 and MIS 11 on the Iberian Margin

Palumbo Eliana ^{1,*}, Voelker Antje H.L. ^{2,3}, Flores Jose Abel ⁴, Amore Ornella F. ⁵

¹ Independent Researcher, Via Roma SNC – Pco Adelaide, 81010 Dragoni, CE, Italy

² Divisão de Geologia e Georecursos Marinhos, Instituto Português do Mar e da Atmosfera (IPMA), Rua Alfredo Magalhães Ramalho 6, 1495-006 Lisboa, Portugal

³ Centre of Marine Sciences (CCMAR), Universidade do Algarve, Campus de Gambelas, 8005-139 Faro, Portugal

⁴ Departamento de Geología, Universidad de Salamanca, 37008 Salamanca, Spain

⁵ Dipartimento di Scienze e tecnologia, Università degli Studi del Sannio, 82100 Benevento, Italy

* Corresponding author : Eliana Palumbo, email address : eliana.palumbol@istruzione.it

Abstract :

Understanding interglacial climate variability is a key issue in the scientific community. Here we compared records from Marine Isotope Stage (MIS) 11 to those from MIS 1 (Holocene) as they are perceived to be possible analogs. Our study on the Iberian Margin, a key area to investigate surface dynamics in the Atlantic Ocean, incorporates coccolithophore assemblage and alkenone data of core MD03–2699 and their statistical analyses. Evaluating similarities between MIS 11 and MIS 1 depends on the way the two MIS are being aligned, i.e. at the deglaciation or based on the precession signal. During the deglaciation of either MIS 12 or MIS 2, the Iberian Margin was affected by abrupt decreases in SST and in coccolithophores' paleoproductivity caused by the arrival of subpolar surface waters. Just prior to the decline, in both the intervals, the Portugal Current affected the studied site, although a possible difference in upwelling strength is here suggested and related to more intense westerlies during the last glacial than the late MIS 12. Similar surface-ocean dynamics occurred at the onset of both MIS 11 and MIS 1 as indicated by the prevalence of the Iberian Poleward Current and sometimes the Azores Current, although the subtropical waters were more oligotrophic during the MIS 2 deglaciation than the MIS 12 one. Synchronizing our records according to the precession cycles aligns the early-to-mid Holocene with the second, warmer phase of MIS 11c. During both these intervals, the western Iberian Margin was mainly affected by the Iberian Poleward Current that transported more temperate-warm, mesotrophic surface waters during MIS 11c than during the early-to-mid Holocene. During the early to mid-Holocene the Iberian Margin endured incursions of colder surface waters that did not occur during MIS 11c allowing us to hypothesize that the studied site experienced, from a paleoceanographic point of view, a more stable period during MIS 11c than the early Holocene. Finally, spectral analysis suggests the role of full, half and fourth precession components in driving surface-ocean variability during MIS 11 and during the last 24 kyr BP.

Highlights

► Comparison of two eccentricity minima interglacials with different duration ► Evaluation of surface-ocean dynamics during MIS 11 vs. MIS 1 off W Iberia ► Both experienced different productivity regimes despite similar surface temperatures. ► Important role of full, half and fourth precession cycles in surface-ocean dynamics.

Keywords : Eccentricity minimum, Coccolithophores, Surface-ocean evolution, Statistical analysis, Precession cycles, Iberian Margin

52 ***1. Introduction***

53 During the last decade, many studies focused on the possible analogy between Marine
54 Isotope Stage (MIS) 11 and the Holocene (Hodell et al., 2000; Loutre, 2003; Loutre and Berger,
55 2003; Rohling et al., 2010; Tzedakis, 2010; Kandiano et al., 2012; Bubenshchikova et al., 2015).
56 Both interglacial periods are characterized by minima in Earth's eccentricity; a particular
57 configuration that occurred only once more during the last 1 Myr, i.e. during MIS 19. On the other
58 hand, precession and obliquity variability during the target period 5 ka Before Present (BP) to 60 ka
59 After Present was not identical to the one of MIS 11 (Loutre and Berger, 2000; 2003). Despite the
60 imperfect match in the orbital parameters' configuration, MIS 11 and MIS 1 show a high analogy in
61 terms of the insolation signal with similar values of atmospheric (pre-human activity) CO₂
62 concentrations (Loutre and Berger, 2000; 2003 and references therein). Although attention shifted
63 to other possible analogs during the last years, such as MIS 19 (Pol et al., 2010; Tzedakis et al.,
64 2012; Emanuele et al., 2015; Ferretti et al., 2015), the scientific discussion on MIS 11 is still
65 ongoing (e.g., Candy et al., 2014; Bubenshchikova et al., 2015; Maiorano et al., 2015; Oliveira et
66 al., 2016; Saavedra-Pellitero et al., 2017; Marino et al., 2018). While not often mentioned in this
67 context, other interglacials (i.e., MIS 5e, 9e, 15a, 15e) also show this phasing, but with varying
68 amounts of precessional power and obliquity amplitude (Yin and Berger, 2010).

69 In order to understand possible analogies also in terms of common evolution, different
70 alignment techniques were previously proposed. The first option is based on insolation and orbital
71 parameters, whereby the June insolation signals through precessional variations are aligned
72 following Loutre and Berger (2000, 2003). The second option, used by the EPICA Community
73 Members (2004) for the EPICA Dome C (EDC) Antarctic ice core, lines up Terminations I and V
74 using obliquity sinusoidal curves. Tzedakis (2010) compared southern European tree populations
75 during MIS 11 and MIS 1 using the criteria of obliquity and precession alignments. Rohling et al.
76 (2010) used the alignment method of sea-level signal synchronization. In any case, when MIS 11c
77 is compared to the Holocene we have to take into account that MIS 11c appears to be an
78 exceptionally long interglacial, generally with a 2–3 times longer duration than the Holocene (Past
79 Interglacials Working Group of PAGES, 2016). The MIS 11c duration is also longer than many of
80 the other interglacials, none of which (except for MIS 13, see below) have mean durations twice as
81 long as the Holocene (Past Interglacials Working Group of PAGES, 2016).

82 Because of the keen interest in MIS 11 climate evolution, studies exist from different areas
83 and from continental and marine archives (e.g., Ayling et al., 2015; Benardout, 2015; Candy et al.,
84 2014; Cheng et al., 2016; D’Anjou et al., 2013; Fawcett et al., 2011; Milker et al., 2013; Antoine et
85 al., 2016; Regattieri et al., 2016; Reyes et al., 2014; Stepanchuk and Moigne, 2016; Saavedra-
86 Pellitero et al., 2017). Accordingly, an increasing number of deep-sea cores provided insights into
87 surface-ocean dynamics (e.g., Dickson et al., 2010; Voelker et al., 2010; Kandiano et al., 2012;
88 Vázquez Riveiros et al., 2013; Maiorano et al., 2015; Saavedra-Pellitero et al., 2017), including on
89 the Iberian Margin (Rodrigues et al., 2011, 2017; Amore et al., 2012; Palumbo et al., 2013a;
90 Oliveira et al., 2016; Sánchez-Goñi et al., 2016). Due to the high sedimentation rate, which allows
91 detecting millennial-to-centennial scale variability, the Iberian Margin is considered a key area for
92 paleoclimate studies (e.g., Shackleton et al., 2000; Hodell et al., 2013). In addition, this area is
93 oceanographically characterized by the Portugal-Current System and seasonal upwelling (Ríos et
94 al., 1992; Fiúza et al., 1998; Pérez et al., 2001; Coelho et al., 2002; Peliz et al., 2005; Relvas et al.,
95 2007).

96 The Iberian Margin has been intensely studied over the last two decades in order to better
97 understand late Quaternary glacial-interglacial and millennial-scale climate variability (e.g., Skinner
98 et al., 2003; Eynaud et al., 2009; Amore et al., 2012; Hodell et al., 2013; Margari et al., 2014;
99 Marino et al., 2014; Oliveira et al., 2016; Salgueiro et al., 2010; Shackleton et al., 2000; Voelker et
100 al., 2010). Several studies provided detailed Sea-Surface Temperature (SST) and paleoproductivity
101 reconstructions for MIS 11 and MIS 1 and discussed their relationships to surface-ocean dynamics

102 (Rodrigues et al., 2010; Rodrigues et al., 2011, 2017; Amore et al., 2012; Palumbo et al., 2013a, b;
103 Marino et al., 2014; Maiorano et al., 2015).

104 Our choice to use coccolithophores as paleoclimate proxy is related to their ability in
105 recording the smallest climatic fluctuations thanks to their sensitive response to SST, nutrient
106 availability, salinity, and sunlight changes (e.g., McIntyre and Bé, 1967; Baumann and Freitag,
107 2004; Moita et al., 2010; Poulton et al., 2017; Guerreiro et al., 2017; Ausin et al., 2018). Previous
108 studies demonstrated their role to reconstruct changes in the main surface-ocean currents off
109 Portugal, in particular in combination with alkenones data (Amore et al., 2012; Palumbo et al.,
110 2013a, b). The main aim of our study is defining possible analogies between the dynamics that led
111 from the glacials to the interglacials and the evolution of the full interglacial conditions focusing on
112 the characteristics of the main surface ocean currents affecting our study site. Previous studies of
113 the coccolithophore assemblages revealed different structures depending on the prevailing surface-
114 ocean currents and thus nutrient availability and SST during the middle and late Pleistocene to
115 Holocene (Amore et al., 2012; Palumbo et al., 2013a, b). Whereas the species *Emiliana huxleyi*
116 dominates the late glacial to Holocene assemblage (Palumbo et al., 2013a), MIS 11 falls into the
117 acme of *Gephyrocapsa caribbeanica* (Amore et al., 2012; Palumbo et al., 2013b), both species
118 belonging to the Noelaerhabdaceae family. *E. huxleyi*, a cosmopolitan species, can tolerate large
119 temperatures ranges and both eutrophic and oligotrophic conditions (Okada and McIntyre, 1979;
120 Winter et al., 1994). The paleoecology of *G. caribbeanica* is still under discussion. Its dominance, a
121 global and synchronous event (e.g., Flores et al., 1999, 2003; Baumann and Freitag, 2004), could
122 potentially be caused by a rapid phylogenetic evolution.

123 In this study, we evaluate possible similarities or differences in surface-ocean changes and
124 their impact on coccolithophores during MIS 11 against MIS 1 using previously published
125 coccolithophore assemblage data (Amore et al., 2012; Palumbo et al., 2013a, b) from sediment core
126 MD03-2699 (Fig. 1). We re-analyze the data with statistical analyses, in particular principal
127 component analysis (PCA), to better quantify the relationships between coccolithophore species and
128 environmental conditions. Assessing conditions during these particular periods helps evaluating if
129 one of the MIS 11/MIS 1 alignments fits better with the coccolithophores' evidence or if a
130 compromise between both solutions is needed.

131

132 **2. Regional Setting**

133 Sediment core MD03-2699 (39°02.20'N, 10°39.63'W) was recovered on the Estremadura
134 promontory off central Portugal (Fig. 1). In this region, the hydrography is connected to the
135 Portugal Current System and strongly influenced by the seasonal and intra-seasonal migrations of

136 the Azores High pressure center. The Portugal Current System was described in detail in previous
137 studies (Ríos et al., 1992; Fiúza et al., 1998; Pérez et al., 2001; Coelho et al., 2002; Peliz et al.,
138 2005; Relvas et al., 2007). All the system's main currents share a common link to the Gulf Stream
139 waters with the subtropical gyre's southwestward recirculation, i.e. the Portugal Current, branching
140 off from the North Atlantic Current (Fig. 1). The Azores Current, a unique current crossing the
141 North Atlantic's subtropical gyre near 34°N, branches off directly from the Gulf Stream (Klein and
142 Siedler, 1989) and can thus transport low latitude signals directly to the Iberian margin. The mixed
143 surface waters between the North Atlantic Current and the Azores Current are sometimes referred to
144 as the North Atlantic Transitional Waters (Schwab et al., 2012).

145 During spring/summer, the pressure cell of the Azores High moves northward leading to an
146 intensification of the westerly winds. This activates upwelling on the western Iberian margin and
147 leads to the prevalence of the cool, less saline and nutrient-rich Portugal Current in the study area
148 (Fig. 1a). The southward migration of the Azores High during autumn/winter causes a reduction of
149 westerly winds' intensity, which favors the northward flow of the warm, salty and nutrient-poor
150 Iberian Poleward Current over the area (Fig. 1b). The Portugal Current transports Eastern North
151 Atlantic Central Waters (ENACW) of subpolar origin (ENACWsp; Fig. 1a) southward, which
152 usually flows below its subtropical counterpart, ENACWst, transported northward by the Iberian
153 Poleward Current (Fig. 1b). The Iberian Poleward Current is seen as a northern branch of the
154 Azores Current (Peliz et al., 2005; Fig. 1).

155 The Azores High also experiences intra-seasonal variability, in particular during winter,
156 which is reflected in the North Atlantic Oscillation (NAO; Hurrell, 1995), the most relevant
157 atmospheric phenomenon in the North Atlantic sector. Negative values of the NAO index indicate a
158 reduced pressure gradient between the Azores High and Icelandic Low (Hurrell, 1995; Fig. 1). This
159 atmospheric setting leads to a reduction of the westerlies over the eastern North Atlantic (Trigo et
160 al., 2004), to generally warm conditions over Iberia (Hurrell and Deser, 2010) and to an
161 intensification of the Iberian Poleward Current (Sánchez et al., 2007). Positive modes of the NAO
162 correspond to an increased pressure gradient causing generally cold conditions and a strengthening
163 of the westerlies and of the upwelling off Iberia (Hurrell, 1995; Sánchez et al., 2007; Hurrell and
164 Deser, 2010).

165

166 **3. Material and Methods**

167 **3.1 *Coccolithophore assemblages and alkenones***

168 For the initial assemblage analyses (Amore et al., 2012; Palumbo et al., 2013a, b), 219
169 samples were analyzed for the MIS 12 to MIS 11 interval (445–360 kyr) and 150 samples for the

170 MIS 2 to MIS 1 interval. In both intervals, sample spacing was 2 cm leading to a temporal
171 resolution of about 0.4 kyr in the MIS 12 to MIS 11 interval and of about 0.140 kyr during the last
172 24 kyr BP. With the exception of the *Umbilicosphaera sibogae* record for the MIS 12-MIS 11
173 period, which is here published for the first time, we re-analyzed these published data. The MD03-
174 2699 samples for coccolithophore assemblages were prepared following Flores and Sierro (1997).
175 Details on the assemblage analyses are provided in Palumbo et al. (2013a, b). Total abundance or
176 abundance of a particular taxon is expressed as number of coccoliths per gram of sediment
177 (#coccoliths/g of sediment) or as relative abundance (%). Fluxes are presented as Nannofossil
178 Accumulation Rate (NAR, #coccoliths/g of sediment*cm⁻²*kyr⁻¹). Due to their ecological
179 sensitivity to specific marine environmental factors, selected coccolithophore taxa or group of taxa
180 have been identified as good indicators for the main surface-ocean currents characterizing the
181 Portugal Current System (Table 1) (Amore et al., 2012; Palumbo et al., 2013a, b). The alkenone
182 based data (SST, C_{37:4}%) were originally published in Rodrigues et al. (2010, 2011) and Palumbo et
183 al. (2013a) and their paleoceanographic implications are listed in table 1.

184

185 **3.2 Alignments of the Marine Isotope Stages**

186 For extricating potential analogies in the surface currents' evolution between MIS 11 and
187 MIS 1 (Holocene) off the Iberian Margin, correctly aligning the records of both periods is essential.
188 Different options exist to align the two MIS and each version has implications for comparing the
189 two MIS and for predicting a possible length of the current interglacial.

190 Figure 2 shows the two different approaches tested in this paper based on the SST data: we
191 use 1) the termination/deglaciation alignment and 2) the precession alignment. When the
192 deglaciations are considered as tie point, the pronounced SST drops during Terminations V and I
193 are lined up, i.e. Heinrich-type event 4 (between 428 and 427 ka; Rodrigues et al., 2011) with the
194 18-15 ka BP interval (Rodrigues et al., 2010). Following the precession synchronization criterion,
195 the SST records were aligned comparing the second half of MIS 11c, i.e. the one coinciding with
196 the sea-level highstand, with the early-to-mid Holocene.

197

198 **3.3 Age models**

199 In this study, we use the age models previously published for core MD03-2699. The age
200 model for the MIS 1 to MIS 2 interval (Rodrigues et al., 2010) is based on calibrated ¹⁴C ages
201 during the Holocene and a correlation between the SST records of cores MD03-2699 and MD01-
202 2444 (Martrat et al., 2007) during the glacial period. The mid-Brunhes chronology (Voelker et al.,
203 2010) was established by relating the benthic δ¹⁸O record of core MD03-2699 to the one of ODP

204 Site 980 (McManus et al., 1999) on its LR04 chronology (Lisiecki and Raymo, 2005). The average
205 sedimentation rate is 14 cm/kyr for the MIS 1 interval and ~6 cm/kyr for MIS 11.

206

207 **3.4 Statistical analyses**

208 Principal Components Analysis (PCA), a tool included in the software PAleontological
209 Statistics (PAST; Hammer et al., 2001), was applied to three time intervals: 1) the complete time
210 series of the respective interval; 2) the full interglacial period; and 3) the deglacial interval. PCA
211 finds hypothetical variables (components) accounting for as much as possible of the variance in
212 multivariate data (Davis, 1986; Harper, 1999) that are linear combinations of original variables
213 (Hammer et al., 2001). The most important components are correlated with other underlying
214 variables that in the case of ecological data can be a physical gradient (Hammer et al., 2001). The
215 PCA usually allows assessing the eigenvalues and eigenvectors of the variance-covariance matrix or
216 the correlation matrix. Our study case is represented by a dataset composed of variables measured
217 in different units; so, we used the correlation method because this way the variables are
218 automatically normalized by the program (Hammer et al., 2001). The tool also allows estimating the
219 percentages of variance accounted for by the principal components. The analysis is usually
220 significant when the variance is accounted for by the first one or two components (Hammer et al.,
221 2001). In some cases, our results are also coherent for the third component because the component
222 can clearly be linked to a particular oceanographic feature.

223 In addition, spectral analysis was performed using the REDFIT tool implemented in the
224 PAST software (Hammer et al., 2001). We re-analyzed data previously explored by Palumbo et al.
225 (2013b) for MIS 11 using a setting aimed at more details in the higher frequency range (e.g.,
226 periodicities of 5-6 kyr). The same setting was then applied to the MIS 1 coccolith and the alkenone
227 data of both periods, for which a frequency analysis is presented for the first time. The program
228 REDFIT allows analyzing unevenly sampled time series and selecting the number of oversampling
229 and segments to optimize the output of the power spectra. In order to overcome the continuous
230 decrease of spectral amplitude with increasing frequency, typical of paleoclimate dataset, the
231 program allows to apply a first-order autoregressive (AR1) process (“red noise”; Schulz and
232 Mudelsee, 2002). In addition, the spectral significance of the peaks, depending on the segment
233 length (Thomson, 1990), is estimated selecting “critical” false-alarm levels relatively to a fixed set
234 of false-alarm levels (Schulz and Mudelsee, 2002). In our analyses, we set the false-alarm levels to
235 90% and 95% (corresponding to χ^2 90% and χ^2 95%), respectively, and considered as significant –
236 from a paleoceanographic point of view– only those peaks reaching the 95% level or higher.
237 Finally, the bandwidth (BW), indicating the spectral resolution given as the width between the -6dB

238 points (Schulz and Mudelsee, 2002), is 0.080 and 0.021 for the MIS 1 and MIS 11 intervals,
239 respectively.

240

241 **4. Results**

242 **4.1 Alignments of Marine Isotope Stages: Coccolithophore assemblages and alkenone data**

243 The SST curves of both MIS 11 and MIS 1 support the two alignment options (Fig. 2). The
244 deglaciation option aligns the two sharp SST decreases, although the SST reached lower values
245 during MIS 12. Following the precession alignment, the Holocene SST record overlaps with the
246 second MIS 11c SST plateau starting at 410 ka, with both records showing comparable maximum
247 values of 17-18°C and a long-term declining trend.

248 Figures 3 and 4 summarize and compare the most relevant coccolith and alkenone data for
249 the two intervals. Between 445 and 441 ka, i.e., during MIS 12, the NAR of small *Gephyrocapsa*
250 reached maximum values in the order of e^{+10} before declining, whereas total NAR were
251 significantly higher between 23 and 19 ka BP, i.e., during MIS 2, with values in the order of e^{+11}
252 (Fig. 3). During the same periods, the SST show comparable values of about 15°C (Fig. 2). The
253 intervals 440 ka-427 ka and 18-15 ka BP were both marked by highest values of *C. pelagicus* ssp.
254 *pelagicus* and of $C_{37:4}$ % and the lowest values of total NAR and small *Gephyrocapsa* accumulation
255 rate (Fig. 3). Between 425 and 409 ka increased percentage values of *U. sibogae* and *C. pelagicus*
256 ssp. *azorinus* are observed that are comparable to those recorded between 12 and 7 kyr BP, although
257 *C. pelagicus* ssp. *pelagicus* percentages show frequent peaks during the latter phase, which are not
258 recorded during MIS 11c.

259

260 **4.2 Principal Component Analysis (PCA)**

261 PCA was used in this study to evaluate the correlation among several variables. The PCA
262 results for the complete time series and the interglacial and deglacial intervals of each period,
263 respectively, are shown in Figures 5, 6 and 7. The PCA of the last 24 kyr BP interval (Fig. 5A, B),
264 performed on SST, $\%C_{37:4}$, $\%C. pelagicus$ ssp. *pelagicus*, $\%U. sibogae$, and the small
265 *Gephyrocapsa* accumulation rate, reveals that 48% of the variance is represented by principal
266 component (pco) 1, 26% by pco2 and 15% by pco3. The scatter diagrams of pco1 vs. pco2 and pco3
267 vs. pco1, respectively, display similar influences for SST and $\%U. sibogae$ and for $\%C. pelagicus$
268 ssp. *pelagicus* and $\%C_{37:4}$ (Fig. 5A), but an independent influence for the small *Gephyrocapsa*
269 accumulation rate within the 95% ellipse (Fig. 5B). For the 445-360 ka interval, the PCA (Fig. 5C,
270 D) reveals that 42% of the variance is represented by pco1, 21% by pco2 and 16% by pco3, a total
271 of 79%. Minor variance percentages are indicated for pco4 and pco5. The pco1 vs. pco2 scatter

272 diagram shows independent influences for SST and small *Gephyrocapsa* accumulation rate,
273 whereas similar influences are exposed for %*C. pelagicus* ssp. *pelagicus* and %C_{37:4} within the 95%
274 ellipse (Fig. 5C). The pco1 vs. pco3 scatter diagram displays similar influences for SST and %*U.*
275 *sibogae* (Fig. 5D).

276 The PCA performed for the deglacial interval from 19 to 13.5 kyr BP (Fig. 6A) for the
277 parameters of small *Gephyrocapsa* accumulation rate, %*U. sibogae*, SST, %*C. pelagicus* ssp.
278 *pelagicus*, and %C_{37:4} shows 43% of variance for pco1 and 27% for pco2. The pco1 vs. pco2 scatter
279 diagram indicates similar influences for SST and %*U. sibogae* and for %*C. pelagicus* ssp. *pelagicus*
280 and %C_{37:4} (Fig. 6A). An independent behavior is revealed for the small *Gephyrocapsa*
281 accumulation rate (Fig. 6A). The PCA performed on the same proxies for the interval 430-425 kyr
282 (MIS 12 deglaciation; Fig. 6B) results in 49% of variance for pco1 and 20% for pco2. Independent
283 behaviors are observed for all the proxies (Fig. 6B)

284 For the early interglacial MIS 1 interval of 12 to 7 kyr BP, the PCA (Fig. 7A) performed on
285 the small *Gephyrocapsa* accumulation rate, %*U. sibogae* and SST (excluding %*C. pelagicus* ssp.
286 *pelagicus* and %C_{37:4} because of low variability) discloses 49% of variance for pco1 and 30 % for
287 pco2. The pco1 vs. pco2 scatter diagram shows similar influences for SST and %*U. sibogae* and an
288 independent behavior for the small *Gephyrocapsa* accumulation rate (Fig. 7A). PCA performed on
289 the same proxies for the interval 409-402 kyr (Fig. 7B) indicate 62% of variance for pco1 and 29%
290 for pco2 and the pco1 vs. pco2 scatter diagram reveals independent influences for all the proxies
291 (Fig. 7B).

292

293 **4.3 Spectral Analysis**

294 The spectral analyses results for the last 24 kyr BP interval (Fig. 8), reveal significant cycles
295 close to 5-6 kyr in the records of the small *Gephyrocapsa* absolute abundance (#coccoliths/g of
296 sediment; Fig. 8A), sum of cold species (Fig. 8B) and the %*C. pelagicus* spp. *azorinus* (Fig. 8E).
297 These periods are also observed in the %*U. sibogae* periodogram (Fig. 8D), although with a lower
298 significance (reaching 90-95% significance levels). These cycles are not seen at significant levels in
299 the %*C. pelagicus* ssp. *pelagicus* power spectrum (Fig. 8C).

300 For the 445-360 kyr interval, the power spectra for the small *Gephyrocapsa* accumulation
301 rate, %*U. sibogae* and SST reveal cycles close to 10-11 kyr in addition to the 5-6 kyr cycles (Fig.
302 8A, C and D). For the %C_{37:4} periodogram, these cycles are present with a lower significance
303 (reaching 90-95% significance levels; Fig. 8B).

304

305

306 **5. Discussion**

307 **5.1. Indications from the extended time intervals**

308 The PCA results allow to distinguish between the three, main surface-ocean regimes that
309 influenced coccolithophores on the Iberian Margin. During both the MIS 11-MIS 12 and MIS 1-
310 MIS 2 intervals, the first three pco's are sufficient to explain the coccolithophores' characteristics in
311 terms of prevailing SST and nutrient conditions. For the MIS 11-MIS 12 period (Fig. 5C, D), the
312 first two components are related to the nutrient-rich, temperate-warm Portugal Current and to the
313 subpolar waters regime that is portrayed as cold and less adequate for the development of
314 coccolithophores (Fig. 5C). The third pco is connected to the Iberian Poleward Current regime,
315 which at that time is characterized by warm surface waters with no particular relevance to nutrient
316 concentrations (Fig. 5D). In the case of the MIS 1-MIS 2 interval, the first three pco's represent
317 90% of variance (Fig. 5A, B). There, the first two components are linked to the subpolar and Iberian
318 Poleward Current regimes, the latter of the two currents probably transported warm and, in contrast
319 to MIS 11, oligotrophic waters (Fig. 5A). The third pco identifies the Portugal Current regime (Fig.
320 5B). As indicated by the coccolith and alkenone data (Fig. 3), the Portugal Current and the subpolar
321 waters show similar characteristics during both MIS 11 and MIS 1. The Iberian Poleward Current,
322 on the other hand, appears to transport different kinds of waters, distinguished mainly in terms of
323 nutrient availability, i.e. being more mesotrophic during MIS 11 as reflected in the lower
324 abundances of *U. sibogae* and *F. profunda* and fewer appearances of *C. pelagicus azorinus* than
325 during MIS 1 (Fig. 4).

326

327 **5.2 Deglaciations**

328 The most common, extreme events recognized at the Iberian margin during the deglaciations
329 are significant SST minima (Fig. 2; Rodrigues et al., 2017), which in core MD03-2699 are also
330 marked by a $\delta^{13}C_{37:4}$ increase indicating less saline surface waters, a decline in coccolithophore
331 productivity and increased percentages of *Coccolithus pelagicus* ssp. *pelagicus* (Fig. 3) (Rodrigues
332 et al., 2010; 2011; Amore et al., 2012; Palumbo et al., 2013a, b). During the transition from MIS 12
333 to MIS 11 (Heinrich-type event 4) and during the interval 18-15 ka BP (Greenland stadial
334 2a/Heinrich event 1), the Iberian margin was thus characterized by the arrival of cold, fresh surface
335 waters of subpolar origin, which, together with a less intense Portugal Current and reduced wind
336 strength, hampered coccolithophore productivity (Amore et al., 2012; Rodrigues et al., 2011;
337 Palumbo et al., 2013b; Marino et al., 2014).

338 Directly comparing the two deglaciation intervals (Fig. 3) highlights that the period of low
339 paleoproductivity during MIS 12 lasted significantly longer (440-427 ka) than Heinrich-type event

340 4 and thus also longer than the corresponding period during the MIS 2 deglaciation, i.e. Heinrich
341 event 1. Just prior to the arrival of the subpolar waters, the Iberian margin experienced increased
342 paleoproductivity with Portugal Current persistence during MIS 12 and MIS 2 (Amore et al., 2012;
343 Palumbo et al., 2013a, b). However, comparing the paleoproductivity records during the two
344 glacials, reveals some differences in the Portugal Current dynamics as indicated by the order of
345 magnitude difference in the values of the paleoproductivity proxies (Fig. 3). The Portugal Current
346 and associated upwelling regime were more intense during the last glacial maximum than during
347 late MIS 12. Nevertheless, SST values (Fig. 2) were quite comparable during both periods (values
348 close to 15°C), suggesting that the main difference cannot be associated with a response of
349 coccolithophores to different temperature ranges but more likely to higher nutrient availability
350 during MIS 2 than MIS 12, which, at the studied site, is nowadays caused by stronger westerly
351 winds and upwelling intensity (Ríos et al., 1992; Fiúza et al., 1998; Pérez et al., 2001; Coelho et al.,
352 2002; Peliz et al., 2005; Relvas et al., 2007). In fact, the PCA reveals that during both intervals, i.e.
353 19-13.5 kyr BP (Fig. 6A) and 430-425 kyr (Fig. 6B), the paleoproductivity increase occurred during
354 warming phases, whereas the subpolar waters were clearly characterized by low SST and less
355 adequate conditions for coccolithophore proliferation.

356 In addition, the oceanographic signal indicated by the PCA (Fig. 6A, B) during both
357 deglaciations suggests that the two main components, representing 70% and 79% of variance,
358 respectively, are enough to explain the surface-ocean signals. The pco1 vs. pco2 scatter diagram for
359 the interval 19-13.5 kyr BP (Fig. 6A) can be interpreted as function of temperature and nutrient
360 availability allowing to distinguish clearly the three, main surface-ocean regimes affecting the
361 Iberian margin during this interval, i.e. the Portugal Current, the Iberian Poleward Current and the
362 subpolar waters. The pco1 vs. pco2 scatter diagram for the MIS 12 deglaciation (Fig. 6B), on the
363 other hand, can be interpreted as function of temperature and subpolar waters with no distinct
364 nutrient signature.

365 Despite apparently different wind and thus upwelling strengths, surface-ocean dynamics
366 evolved quite similarly during both periods. The Portugal Current persistence at the beginning of
367 the interval was substituted by the arrival of subpolar waters followed by a gradual SST increase
368 associated with a period of higher surface instability. In fact, during the onsets of both MIS 11 and
369 MIS 1, i.e., during the early interglacial phase, the site was affected by the Iberian Poleward Current
370 and sometimes even the Azores Current (Fig. 4). The subtropical water influence alternated with
371 periods of Portugal Current prevalence and decreasing persistence of subpolar waters. The PCA
372 result (Fig. 6A), however, reveals that during the MIS 2 deglaciation the Iberian Poleward Current
373 transported warm, nutrient-poor surface waters, as shown by the co-occurrence of *U. sibogae* with

374 high SST and low nutrient availability. During the MIS 12 deglaciation, on the other hand, the PCA
375 (Fig. 6B) indicates *U. sibogae* coinciding with medium levels of SST and nutrient availability,
376 suggesting that the Iberian Poleward Current transported warm-temperate, mesotrophic surface
377 waters. The hypothesis of more oligotrophy during the MIS 2 deglaciation is also supported by the
378 more frequent and generally more abundant presence of *F. profunda*, a species which is considered
379 to live in stratified surface waters (e.g., Molfino and McIntyre, 1990) (Fig. 4).

380

381 **5.3 MIS 11c vs. early-to-mid Holocene**

382 In the case of aligning the deglaciations, the early-to-mid Holocene (12 – 7 kyr BP) does not
383 show a clear analogy with early MIS 11 (425 – 409 kyr) both in terms of mean SST values and
384 surface-ocean dynamics (Fig. 2). In fact, the early MIS 11 was characterized by mean SST values of
385 <18°C, whereas the early-to-mid Holocene experienced mean values >18°C (Rodrigues et al., 2011;
386 Rodrigues et al., 2010). The early MIS 11 period was marked by Portugal Current prevalence and
387 the upwelled waters were replenished by ENACWst (Palumbo et al., 2013a). In contrast, the Iberian
388 margin was affected mainly by the Iberian Poleward Current during the early-to-mid Holocene
389 (Palumbo et al., 2013b), in agreement with coccolithophore and planktonic foraminifera evidence
390 from the southern and southwestern Iberian margin (e.g., Colmenero-Hidalgo et al., 2004; Salgueiro
391 et al., 2014). The best analogy is reached by comparing the early-to-mid Holocene with the peak
392 interglacial period of MIS 11c (409 – 402 kyr), following the precession alignment criterion (Fig.
393 2). The SST show comparable mean values around 18°C and coccolithophore productivity in both
394 intervals was low, which, in combination with the higher values of *U. sibogae* (Fig. 4), suggests the
395 prevalence of the Iberian Poleward Current. The presence of *C. pelagicus* ssp. *azorinus* indicates
396 that the Azores Current contributed significantly to the Iberian Poleward Current during short
397 episodes (Fig. 4). Both *U. sibogae* and *C. pelagicus* ssp. *azorinus* show maximum percentages
398 during MIS 11c, but lower than the values reached during early MIS 1. *F. profunda* also displays
399 higher percentages during early MIS 1 than during MIS 11c (Fig. 4). All these evidences suggest a
400 stronger Iberian Poleward Current and ENACWst influence leading to stronger stratification during
401 the early-to-mid Holocene. In fact, the PCA (Fig. 7A, B) indicates that the Iberian Poleward Current
402 transported oligotrophic, warm/subtropical waters during the early-to-mid Holocene to the study
403 site, whereas the advected waters were more temperate-warm and mesotrophic during MIS 11c.

404 For the evaluation of the best analog alignment, it is important to comprehend what might
405 have caused the different Iberian Poleward Current properties during the two interglacial periods.
406 Variance in the properties could be related to a different position and/or strengthening of the Azores
407 High as a consequence of two different positions of the Inter-Tropical Convergence Zone (ITCZ).

408 Pervasive relatively warm conditions off SW Iberia may reflect the persistent dominance of the
409 subtropical Azores and Iberian Poleward Currents in this area during the final phase of MIS 11c
410 (Voelker et al., 2010), even after the onset of the northern hemisphere ice sheet growth at ~400 ka
411 (e.g., Oliveira et al., 2016). During both, MIS 11c and the Holocene, the ITCZ moved northward
412 causing a weakening of westerly winds. The ITCZ's position was, however, more southern during
413 MIS 11c relative to the early Holocene (e.g., Kandiano et al., 2012) leading probably to the heat-
414 transport changes within the Iberian Poleward Current. A possible role also of NAO negative-like
415 modes was hypothesized in the general atmospheric setting of MIS 11c (Kandiano et al., 2012). If
416 we consider that negative modes of NAO are nowadays associated to a possible intensification of
417 the Iberian Poleward Current (Sánchez et al., 2007), its intensification during MIS 11c could in
418 effect also be related to similar modes occurring at millennial-scale. Moreover, during the early-to-
419 mid Holocene, between 8.2 and 7 ka BP, the wettest and warmest conditions and indication for
420 NAO variability in terms of higher/lower persistence of the index were documented in southern
421 Spain (Jiménez-Moreno and Anderson, 2012). Regarding the role of NAO+/- modes on the early-
422 to-mid Holocene Azores High/Icelandic Low position, controversial results from paleoclimatic
423 archives have been documented in the last years (Gladstone et al., 2005; Wanner, 2008; Olsen et al.,
424 2012; Morley et al., 2014; Wassenburg et al., 2016), although these patterns do not seem to be a
425 dominant forcing for North Atlantic variability at that time (Repschläger et al., 2017). At the
426 transition from the early to the mid-Holocene, changes in the wind direction could be related to a
427 northward movement of the westerlies (thus their weakening) indicating a northward movement of
428 the Azores High /Icelandic Low cells (Repschläger et al., 2017). We speculate that the possible
429 analogy even so observed in our records could be due to similar mechanisms acting on the
430 atmospheric-surface ocean settings.

431 In addition, throughout the Holocene, *U. sibogae* and paleoproductivity show alternating
432 peaks implying oscillations in the dominant surface-water currents occurring at millennial time-
433 scale, as also proposed for MIS 11 (Palumbo et al., 2013b). The PCA results (Fig. 7) suggest that
434 the first two pco's are enough to explain the two different regimes related to the Portugal and
435 Iberian Poleward Currents, both during the early Holocene and during MIS 11c, confirming a
436 possible Portugal Current prevalence with a general lower amplitude than the Iberian Poleward
437 Current. The Portugal Current, however, exhibits different surface-water characteristics off the
438 Iberian margin. During MIS 11c, the Portugal Current transported nutrient-rich, temperate-warm
439 surface waters, whereas during the early Holocene this current transported more likely cool,
440 nutrient-rich waters. Thus, even if the mean SST values are quite similar, suggesting a similar
441 warming, the two main currents affecting the Iberian margin had distinct characteristics.

442 Although the main signal is represented by the prevalence of the Iberian Poleward Current
443 in both stages, the Iberian margin experienced incursions of colder surface waters during the early
444 to mid-Holocene (Palumbo et al., 2013a; Salgueiro et al., 2014) that did not occur during MIS 11c.
445 The near absence of *C. pelagicus* ssp. *pelagicus* and the $\%C_{37:4}$ values during MIS 11c (Palumbo et
446 al., 2013b; Rodrigues et al., 2011) suggest that the Iberian margin was reached by subpolar waters
447 only during the early Holocene when both of these indicators were observed (Palumbo et al., 2013a).
448 So, our hypothesis is that MIS 11c was, from a paleoceanographic point of view, a more stable
449 period than the early Holocene on the Iberian margin. Pollen data from several European
450 continental records and SST records from the North Atlantic document the occurrence of abrupt
451 events at 410/412 ka and 404 ka, which are related to changes in precipitation or short-term cooling,
452 respectively (e.g., Rodrigues et al., 2011; Koutsodendris et al., 2012; Candy et al., 2014; Kandiano
453 et al., 2017). The variability within MIS 11c was, in fact, more likely associated to a 8.2 ka-type
454 cooling event (e.g., Koutsodendris et al., 2012; Candy et al., 2014). On the other hand, an
455 exceptional event, recognized in the MD03-2699 sediments between 405 and 401 kyr, was probably
456 related to increased river runoff driven by increased precipitation, but lagging evidences of cooling
457 (Palumbo et al., 2013b). Surface-ocean dynamics were not affected as strongly by this variability as
458 the continental climate or coccolithophores and alkenones were not sensitive enough to detect this
459 event, in contrast to the one occurring in the early Holocene.

460

461 **5.3 Role of half and fourth precession cycles**

462 The length of the time window for the last 24 ka BP does not allow investigating full
463 precession cycles, so for this interval we focused only on their half and fourth components
464 characterized by typical periodicity of 10-11 kyr and 5-6 kyr, respectively, as documented by
465 Berger et al. (2006). Regarding to MIS 11, the spectral analysis of the small *Gephyrocapsa*
466 accumulation rate shows the influence on paleoproductivity of full precession cycles but also a
467 possible correlation with its half component (Fig. 9A). The spectral analysis of the *U. sibogae*
468 percentages record indicates the presence of full and fourth harmonic precessional cycles suggesting
469 their role in driving Iberian Poleward Current changes (Fig. 9D). The SST record also reveals an
470 interesting, significant signal in the range of the half-precession cycles (Fig. 9C). The possible role
471 of full precession cycles during the Middle Pleistocene in driving surface-ocean dynamics off the
472 Iberian margin, via their influence on Portugal/ Iberian Poleward Current fluctuations, was
473 previously documented (Amore et al., 2012; Palumbo et al., 2013b) as well as the influence of half
474 and fourth precession components during the transition from MIS 12 to MIS 11 (Palumbo et al.,
475 2013b).

476 The presence of half and fourth precession cycles was predicted in the Equator insolation by
477 Berger et al. (2006), but subsequent studies documented the presence of these cycles also in mid-to-
478 high latitudes marine records (e.g., Weirauch et al., 2008; Ferretti et al., 2010; Amore et al., 2012;
479 Hernández-Almeida et al., 2012; Palumbo et al., 2013b). It is not yet fully understood how marine
480 proxy data at higher latitudes can record high frequency precession cycles within their power
481 spectra. One idea is that mid-to-high latitudes surface-ocean dynamics were driven by changes in
482 insolation at the Equator (Ferretti et al., 2010; Hernandez-Almeida et al., 2012; Palumbo et al.,
483 2013b), even if it is still unclear what is exactly the driving mechanism.

484 Our spectral analysis results indicate that during MIS 11 changes in insolation at the Equator
485 following fourth precession cycles caused variability in the Iberian Poleward Current and led to its
486 intensification off the Iberian margin. In a similar way, half precession cycles via Equator insolation
487 variability caused probably changes in Portugal Current intensification and SST variability. These
488 cycles were also observed in the *C. pelagicus* ssp. *azorinus* power spectrum (Palumbo et al., 2013b)
489 suggesting their possible impact also on the northward flowing branch of the Azores Current, i.e.
490 the Iberian Poleward Current. Regarding the last 24 ka BP data, the fourth precession cycles via
491 insolation at the Equator could be the mechanism behind the Iberian Poleward Current variability
492 off western Iberia as also suggested by the *U. sibogae* power spectrum (Fig. 8D). The fourth
493 component could also be the main forcing for Portugal Current variability and the northward
494 recirculation of the Azores Current as indicated by the power spectra of the small *Gephyrocapsa*
495 absolute abundance (#/g of sediment) and *C. pelagicus* ssp. *azorinus* (Figs. 8A and 8E),
496 respectively.

497 If we consider that the three major currents on the Iberian margin have the Gulf Stream as
498 common source water, a potential transfer mechanism could be that insolation at lower latitudes (in
499 this case the Gulf of Mexico/ Caribbean Sea) caused changes in the source waters of these currents,
500 and as a consequence of oceanic feedbacks these cycles were indirectly recorded in our study area.
501 At the mid (and high) latitudes, in fact, the equatorial currents do not affect the surface
502 oceanography directly, but are linked through the currents arising from them. In addition, because
503 the Iberian margin is under the direct influence of the westerlies controlling the upwelling, a
504 possible influence of Equator insolation on variability in the main North Atlantic atmospheric
505 pressure centers can be supposed.

506 The *C. pelagicus* ssp. *pelagicus* power spectra for both MIS 11 (Palumbo et al., 2013b) and
507 MIS 1 (Fig. 7C) do not show the half and fourth precession cycles' frequencies. Thus, we can
508 interpret these results as an evidence of equatorial insolation not influencing the arrival of subpolar
509 waters at the Iberian margin. However, the power spectrum of the sum of cold species during the

510 MIS 1 interval (Fig. 8B) reveals the presence of fourth precession cycles suggesting their role on
511 the arrival of colder surface waters but not of pure subpolar origin. The most abundant cold species
512 recorded in this interval is represented by *Gephyrocapsa muelleriae* (Palumbo et al., 2013a), which,
513 near the Azores, was used as proxy for the influence of the North Atlantic Transitional Waters
514 during the last 16 kyr BP (Schwab et al., 2012). Our hypothesis is that the North Atlantic
515 Transitional Waters recorded the influence of Equator insolation changes driven by fourth
516 precession cycles as consequence of changes in the North Atlantic, Portugal and Azores Currents.

517 It is also interesting to note that the %C_{37:4} time series for the complete MIS 11 – MIS12
518 interval incorporates significant spectral power close to the periodicities of half and fourth
519 precession components (Fig. 9B). These results suggest that advection of meltwaters was also
520 linked to changes in Equator insolation, potentially via atmosphere-ocean feedbacks at high
521 latitudes. The insolation feedback most likely acted as deteriorating factor on the ice sheets (e.g.,
522 Ruddiman, 2003) and their ice shelf extension, causing, in the end, the arrival of their meltwaters at
523 the studied site.

524

525 **6. Summary and Conclusions**

526 In this study, we compared MIS 11 and MIS 1 coccolithophore and alkenone derived
527 records from core MD03-2699 located on the Iberian margin to search for possible analogies in the
528 temporal evolution of the surface-ocean dynamics. Considering that MIS 11 was an exceptional
529 long interglacial, it is impossible to compare the full interval with entire Holocene trend. So, we
530 opted to compare the records following two main alignment criteria: 1) aligning the deglaciations
531 on the basis of MD03-2699 SST records and 2) aligning based on the precession cycles. We applied
532 PCA to the data with the aim to distinguish possible differences or analogies between the
533 characteristics of the surface water masses affecting the site, in particular in regard to SST and
534 nutrient availability. When aligning the deglaciations, both MIS 12 and MIS 2 experienced the same
535 surface-ocean evolution, namely a productive period being interrupted by the arrival of subpolar
536 waters and then followed by variable conditions during the transition into full interglacial
537 conditions. Even if the general evolutions were similar, the direct comparison highlighted that
538 during the productive periods upwelling was stronger during MIS 2, thereby providing more
539 nutrients for the coccolithophore community. The period of instability at the onset of the
540 interglacials was marked by the reoccurring presence of the Iberian Poleward Current, sometimes
541 with significant contributions from the Azores Current. When applying the precession cycle
542 alignment, our records show the best analogy between early-to-mid Holocene and MIS11c. Also,
543 these periods were characterized by the persistent presence of the Iberian Poleward Current, along

544 with ENACWst. However, the MIS 11c subtropical surface waters were poorer in nutrients
545 (mesotrophic) than their more oligotrophic MIS 1 counterparts. Another important observation that
546 arose from comparing the two interglacial periods is related to the sporadic advection of cold,
547 subpolar surface waters to the Iberian margin. Arrival of such waters was more relevant and
548 frequent during the early-to-mid Holocene than during MIS 11c. Thus, despite the general
549 similarities neither alignment results in exactly the same evolution in the prevailing surface-water
550 masses. So, in conclusion, a compromise between the two solutions proposed here would be the
551 best solution when comparing MIS 1 and MIS 11.

552 Even if during eccentricity minima stages, precession is typically characterized by weak
553 variations (Hilgen et al., 1995, 2003; Zeeden et al., 2013), as it is the case for MIS 11 and MIS 1,
554 our data suggest that this orbital parameter played an important role in surface-ocean dynamics on
555 the Iberian margin. Because of the high resolution of our time series, we could investigate not only
556 the full precession cycles during MIS 11, but also their higher frequency components during both
557 MIS providing additional information on possible analogies/differences of these two crucial stages.
558 From our point of view, it would be interesting to extend the current study to other sites within the
559 North Atlantic's subtropical gyre in order to better understand possible relationships between the
560 main currents and potential influences of the higher frequency precession cycles on the water mass
561 properties and plankton communities.

562

563

564 **Acknowledgements**

565 For the initial work, E. Palumbo was supported by Ph. D. grants provided by MIUR
566 (Ministero dell'Istruzione, dell'Università e della Ricerca). F. O. Amore received financial aid from
567 FRA grants AMORE2013 and AMORE2014. A. Voelker acknowledges financial support from the
568 Fundação para a Ciência e a Tecnologia (FCT) in form of the PORTO project
569 (PDCT/MAR/58282/2004) and her FCT Investigador contract (IF/01500/2014). Recovery of core
570 MD03-2699 during the Picabia cruise onboard the R/V Marion Dufresne (A.V.) was funded by a
571 EU grant of Access to Research Infrastructure. We thank the two anonymous reviewers for their
572 comments that helped to improve our manuscript.

573

574 **Data availability**

575 All proxy data is available from the PANGAEA data center:

576 0-24 ka coccoliths: <https://doi.org/10.1594/PANGAEA.836238>

577 0-24 ka alkenones: <https://doi.org/10.1594/PANGAEA.761812>

578 360-445 ka coccoliths: <https://doi.org/10.1594/PANGAEA.833636> and

579 <https://doi.org/10.1594/PANGAEA.836259>;

580 360-445 ka alkenones: <https://doi.org/10.1594/PANGAEA.761771>

581

582 **References**

583 Amore, F. O., Flores, J.A., Voelker, A. H. L., Lebreiro, S. M., Palumbo, E., and Sierro, F. J.,
584 2012. A Middle Pleistocene Northeast Atlantic Coccolithophore Record: Paleoclimatology and
585 Paleoproductivity aspects. *Marine Micropaleontology*, 90-91, 44-59.

586 Antoine, P., Moncel, M. H., Limondin-Lozouet, N., Loch, J. L., Bahain, J. J., Moreno, D.,
587 Voinchet, P., Auguste, P., Stoetzel, E., Dabkowski, J., Bello, S. M., Parfith, S. A., Tombret, O., and
588 Hardy, B., 2016. Palaeoenvironment and dating of the Early Acheulean localities from the Somme
589 River basin (Northern France): New discoveries from the High Terrace at Abbeville-Carrière
590 Carpentier. *Quaternary Science Reviews*, 149, 338-371, doi: 10.1016/j.quascirev.2016.07.035.

591 Ausín, B., Zúñiga, D., Flores, J.A., Cavaleiro, C., Froján, M., Villaceros-Robineau, N.,
592 Alonso-Pérez, F., Arbones, B., Santos, C., de la Granda, F., G. Castro, C., Abrantes, F., Eglinton,
593 T.I., and Salgueiro, E., 2018. Spatial and temporal variability in coccolithophore abundance and
594 distribution in the NW Iberian coastal upwelling system. *Biogeosciences* 15, 245-262.

595 Ayling B. F., Chappell J., Gagan M. K., and McCulloch M. T., 2015. ENSO variability
596 during MIS 11 (424–374 ka) from *Tridacna gigas* at Huon Peninsula, Papua New Guinea. *Earth
597 and Planetary Science Letters*, 431 (1), 236-246, doi: 10.1016/j.epsl.2015.09.037.

598 Baumann, K.H., and Freitag, T., 2004. Pleistocene fluctuations in the northern Benguela
599 Current system as revealed by coccolith assemblages, *Marine Micropaleontology*, 52 (1-4), 195-
600 215, doi: 10.1016/j.marmicro.2004.04.011.

601 Benardout G., 2015. Ostracod-based palaeotemperature reconstructions for MIS 11 human
602 occupation at Beeches Pit, West Stow, Suffolk, UK. *Journal of Archaeological Science*, 54, 421-
603 425, doi: 10.1016/j.jas.2014.07.027.

604 Berger, A., M. F. Loutre, and Mélice, J. L., 2006. Equatorial insolation: from precession
605 harmonics to eccentricity frequencies, *Climate of the Past*, 2, 131-136, doi: 10.5194/cp-2-131-2006.

606 Brand, L. E., 1994. Physiological ecology of marine coccolithophores, in, *Coccolithophores*,
607 edited by Winter A., and W. Siesser, Cambridge University Press, Cambridge, pp. 39-49.

608 Bréhéret, J., 1978. Formes nouvelles quaternaires et actuelles de la famille des
609 Gephyrocapsaceae (Coccolithophorides), *Comptes Rendus Hebdomadaires des Séances de
610 l'Académie des Sciences Paris*, 287, 447-449.

611 Bubenshchikova N., Nürnberg D., and Tiedemann R., 2015. Variations of Okhotsk Sea
612 oxygen minimum zone: Comparison of foraminiferal and sedimentological records for latest MIS
613 12–11c and latest MIS 2–1. *Marine Micropaleontology*, 121, 52-69, doi:
614 10.1016/j.marmicro.2015.09.004.

615 Buckley, M. W., and Marshall, J., 2016. Observations, inferences, and mechanisms of
616 Atlantic Meridional Overturning Circulation variability: A review. *Rev. Geophys.*, 54, 5-63,
617 doi:10.1002/2015RG000493.

618 Buzas, M. A., 1990. Another look at confidence limits for species proportions. *Journal of*
619 *Paleontology* 64, 842-843.

620 Candy I., Schreve D. C., Sherriff J., and Tye G. J., 2014. Marine Isotope Stage 11:
621 Palaeoclimates, palaeoenvironments and its role as an analogue for the current interglacial. *Earth-*
622 *Science Reviews*, 128, 18-51, doi:10.1016/j.earscirev.2013.09.006.

623 Cheng, H., Edwards, R.L., Sinha, A., Spötl, C., Yi, L., Chen, S., Kelly, M., Kathayat, G.,
624 Wang, X., Li, X., Kong, X., Wang, Y., Ning, Y., and Zhang, H., 2016. The Asian monsoon over the
625 past 640,000 years and ice age terminations. *Nature* 534, 640-646.

626 Coelho, H.S., R. J. J. Neves, M. White, P. C. Leitão, and A. J. Santos, 2002. A model for
627 ocean circulation on the Iberian coast. *Journal of Marine Systems*, 32 (3-4), 153-179.

628 Colmenero-Hidalgo, E., Flores, J. A., Sierro, F. J., Barcena, M. A., Löwemark, L.,
629 Schönfeld, J., and Grimalt, J. O., 2004. Ocean-surface water response to short-term climate changes
630 revealed by coccolithophores from the Gulf of Cadiz (NE Atlantic) and Alboran Sea (W
631 Mediterranean). *Paleogeography Paleoclimatology Paleoecology*, 205 (3-4), 317-336, doi:
632 10.1016/j.palaeo.2003.12.014.

633 D'Anjou, R.M., Wei, J.H., Castañeda, I.S., Brigham-Grette, J., Petsch, S.T., and Finkelstein,
634 D.B., 2013. High-latitude environmental change during MIS 9 and 11: biogeochemical evidence
635 from Lake El'gygytyn, Far East Russia. *Clim. Past* 9, 567-581.

636 Davis, J.C., 1986. *Statistics and Data Analysis in Geology*. John Wiley & Sons, 639 p.

637 Dickson, A.J., Leng, M.J., Maslin, M.A., Sloane, H.J., Green, J., Bendle, J.A., McClymont,
638 E.L., and Pancost, R.D., 2010. Atlantic overturning circulation and Agulhas leakage influences on
639 southeast Atlantic upper ocean hydrography during marine isotope stage 11. *Paleoceanography*,
640 25(3), PA3208, doi: 10.1029/2009pa001830.

641 Emanuele D., Ferretti P., Palumbo E., and Amore F. O., 2015. Sea-surface dynamics and
642 palaeoenvironmental changes in the North Atlantic Ocean (IODP Site U1313) during Marine
643 Isotope Stage 19 inferred from coccolithophore assemblages. *Palaeogeography, Palaeoclimatology,*
644 *Palaeoecology*, 430, 104-117, doi: 10.1016/j.palaeo.2015.04.014.

645 EPICA Community Members. Eight glacial cycles from an Antarctic ice core. *Nature*, 429,
646 623-628, doi: 10.1038/nature02599.

647 Eynaud, F., de Abreu, L., Voelker, A., Schönfeld, J., Salgueiro, E., Turon, J. L., Penaud, A.,
648 Toucanne, S., Naughton, F., Sánchez Goñi, M. F., Malaizé, B., and Cacho, I., 2009. Position of the
649 Polar Front along the western Iberian margin during key cold episodes of the last 45 ka. *Geochem.*
650 *Geophys. Geosyst.*, 10, Q07U05, doi: 10.1029/2009GC002398

651 Fawcett, P.J., Werne, J.P., Anderson, R.S., Heikoop, J.M., Brown, E.T., Berke, M.A., Smith,
652 S.J., Goff, F., Donohoo-Hurley, L., Cisneros-Dozal, L.M., Schouten, S., Sinninghe Damste, J.S.,
653 Huang, Y., Toney, J., Fessenden, J., WoldeGabriel, G., Atudorei, V., Geissman, J.W., and Allen,
654 C.D., 2011. Extended megadroughts in the southwestern United States during Pleistocene
655 interglacials. *Nature* 470, 518-521.

656 Ferretti P., Crowhurst S. J., Naafs B. D. A., and Barbante C., 2015. The Marine Isotope
657 Stage 19 in the mid-latitude North Atlantic Ocean: astronomical signature and intra-interglacial
658 variability. *Quaternary Science Reviews*, 108, 95-110, doi: 10.1016/j.quascirev.2014.10.024.

659 Ferretti, P., Crowhurst, S. J., Hall, M. A., and Cacho, I., 2010. North Atlantic millennial-
660 scale variability 910 to 790 ka and the role of the equatorial insolation forcing. *Earth, and Planetary*
661 *Science Letters*, 293 (1-2), 28-41, doi: 10.1016/j.epsl.2010.02.016.

662 Fiuza, A. F. G., Hamann, M., Ambar, I., Díaz del Río, G., González, N., and Cabanas, J. M.,
663 1998. Water masses and their circulation off western Iberia during May 1993. *Deep Sea Research I*,
664 45 (7), 1127-1160, doi: 10.1016/S0967-0637(98)00008-9.

665 Flores, J. A., and Sierro F. J., 1997. Revised technique for calculation of calcareous
666 nannofossils accumulation rates. *Micropaleontology*, 43 (3), 321-324.

667 Flores, J. A., Sierro, F. J., Frances, G., Vazquez, A., and Zamarreno, I., 1997. The last
668 100,00 years in the western Mediterranean: sea surface water and frontal dynamics as revealed by
669 coccolithophores. *Marine Micropaleontology* 29, 351-366.

670 Flores, J.A., Gersonde, R., Sierro, F.J., 1999. Pleistocene fluctuations in the Agulhas Current
671 Retroflexion based on the calcareous plankton record. *Marine Micropaleontology*, 37(1), 1-22. doi:
672 10.1016/S0377-8398(99)00012-2.

673 Flores, J.-A., Marino, M., Sierro, F.J., Hodell, D.A. and Charles, C.D., 2003. Calcareous
674 plankton dissolution pattern and coccolithophore assemblages during the last 600 kyr at ODP Site
675 1089 (Cape Basin, South Atlantic): paleoceanographic implications. *Palaeogeography,*
676 *Palaeoclimatology, Palaeoecology*, 196(3-4), 409-426.

677 Flores, J. A., Colmenero-Hidalgo, E., Mejia-Molina, A. E., Baumann, K.-H., Henderiks, J.,
678 Larsson, K., Prabhu, C. N., Sierro, F. J., and Rodrigues, T., 2010. Distribution of large *Emiliania*

679 *huxleyi* in the Central and Northeast Atlantic as a tracer of surface ocean dynamics during the last
680 25,000 years. *Marine Micropaleontology*, 76 (3-4), 53-66, doi: 10.1016/j.marmicro.2010.05.001.

681 Gladstone, R. M., Ross, I., Valdes, P. J., Abe-Ouchi, A., Braconnot, P., Brewer, S.,
682 Kageyama, M., Kitoh, A., Legrande, A., Marti, O., Ohgaito, R., Otto-Bliesner, B., Peltier, W. R.,
683 and Vettoretti, G., 2005. Mid-Holocene NAO: A PMIP2 model intercomparison. *Geophysical*
684 *Research Letters*, 32, L16707, doi:10.1029/2005GL023596.

685 Guerreiro, C.V., Baumann, K.H., Brummer, G.J.A., Fischer, G., Korte, L.F., Merkel, U., Sá,
686 C., de Stigter, H., and Stuut, J.B.W., 2017. Coccolithophore fluxes in the open tropical North
687 Atlantic: influence of thermocline depth, Amazon water, and Saharan dust. *Biogeosciences* 14,
688 4577-4599.

689 Hammer, Ø., Harper, D.A.T., Ryan, P.D., 2001. PAST – Palaeontological Statistics.
690 <http://www.toyen.uio.no/~ohammer/past>.

691 Harper, D.A.T. (ed.), 1999. *Numerical Palaeobiology*. John Wiley & Sons, 468 p.

692 Hernández-Almeida, I., Sierro, F. J., Cacho, I., Flores, J. A., 2012. Impact of suborbital
693 climate changes in the North Atlantic on ice sheet dynamics at the Mid-Pleistocene Transition.
694 *Paleoceanography*, 27, PA3214, doi:10.1029/2011PA002209.

695 Hilgen, F. J., Abdul Aziz, H., Krijgsman, W., Raffi, I., and Turco, E., 2003. Integrated
696 stratigraphy and astronomical tuning of the Serravallian and lower Tortonian at Monte dei Corvi
697 (Middle–Upper Miocene, northern Italy). *Palaeogeography, Palaeoclimatology, Palaeoecology*, 199
698 (3–4): 229-264, doi: 10.1016/S0031-0182(03)00505-4.

699 Hilgen, F. J., Krijgsman, W., Langereis, C. G., Lourens, L. J., Santarelli, A., and
700 Zachariasse, W.J., 1995. Extending the astronomical (polarity) time scale into the Miocene. *Earth*
701 *and Planetary Science Letters*, 136 (3–4), 495-510, doi: 10.1016/0012-821X(95)00207-S.

702 Hodell, D. A., Charles, C. D., and Ninnemann, U. S., 2000. Comparison of interglacial
703 stages in the South Atlantic sector of the Southern Ocean for the past 450 kyr: implications for
704 Marine Isotope Stage (MIS) 11. *Global and Planetary Change*, 24(1), 7-26, doi: 10.1016/S0921-
705 8181(99)00069-7.

706 Hodell, D., Crowhurst, S., Skinner, L., Tzedakis, P.C., Margari, V., Channell, J.E.T.,
707 Kamenov, G., Maclachlan, S., and Rothwell, G., 2013. Response of Iberian Margin sediments to
708 orbital and suborbital forcing over the past 420 ka. *Paleoceanography*, 28, 185-199,
709 doi:10.1002/palo.20017.

710 Hurrell, J. W., 1995. Decadal trends in the North Atlantic Oscillation: Regional temperatures
711 and precipitation, *Science*, 269, 676-679, doi: 10.1126/science.269.5224.676.

712 Hurrell, J. W., and Deser, C., 2010. North Atlantic climate variability: The role of the North
713 Atlantic Oscillation. *Journal of Marine Systems*, 79(3–4), 231-244, doi:
714 10.1016/j.jmarsys.2009.11.002.

715 Jiménez-Moreno, G., and Anderson, R. S., 2012. Holocene vegetation and climate change
716 recorded in alpine bog sediments from the Borreguiles de la Virgen, Sierra Nevada, southern Spain.
717 *Quaternary Research*, 77(1), 44-53, doi: 10.1016/j.yqres.2011.09.006.

718 Kandiano E. S., Bauch H. A., Fahl K., Helmke J. P., Röhl U., Pérez-Folgado M., and Cacho
719 I., 2012. The meridional temperature gradient in the eastern North Atlantic during MIS 11 and its
720 link to the ocean–atmosphere system. *Palaeogeography, Palaeoclimatology, Palaeoecology*, 333-
721 334: 24-39, doi: 10.1016/j.palaeo.2012.03.005.

722 Kandiano, E.S., van der Meer, M.T.J., Schouten, S., Fahl, K., Sinninghe Damsté, J.S.,
723 Bauch, H.A., 2017. Response of the North Atlantic surface and intermediate ocean structure to
724 climate warming of MIS 11. *Scientific Reports*, 7, 46192, doi: 10.1038/srep46192.

725 Klein, B., and Siedler, G., 1989. On the origin of the Azores Current. *Journal of Geophysical*
726 *Research*, 94(C5), 6159-6168.

727 Koutsodendris, A. P.,ross, J., Müller, U.C., Brauer, A., Fletcher, W.J., Kühl, N., Kirilova, E.,
728 Verhagen, F.T.M., Lücke, A., and Lotter, A.F., 2012. A short-term climate oscillation during the
729 Holsteinian interglacial (MIS 11c): An analogy to the 8.2ka climatic event? *Global and Planetary*
730 *Change*, 92-93, 224-235.

731 Lisiecki, L. E., and Raymo, M. E., 2005. A Pliocene-Pleistocene stack of 57 globally
732 distributed benthic $\delta^{18}\text{O}$ records. *Paleoceanography*, 20, PA1003, doi:10.1029/2004PA001071.

733 Lopez-Otalvaro, G. E., Flores, J. A., Sierro, F. J., and Cacho, I., 2008. Variations in
734 Coccolithophorids production in the Eastern Equatorial Pacific at ODP Site 1240 over the last seven
735 glacial–interglacial cycles. *Marine Micropaleontology*, 69(1), 52–69, doi:
736 10.1016/j.marmicro.2007.11.009

737 Loutre M. F., and Berger A., 2000. Future Climatic Changes: Are We Entering an
738 Exceptionally Long Interglacial? *Climatic Change*, 46, 61-90, doi: 10.1023/A:1005559827189.

739 Loutre, M. F., 2003. Clues from MIS 11 to predict the future climate – a modelling point of
740 view. *Earth and Planetary Science Letters*, 212(1–2), 213-224, doi:10.1016/S0012-821X(03)00235-
741 8.

742 Loutre, M.F., and Berger, A., 2003. Marine Isotope Stage 11 as an analogue for the present
743 interglacial. *Global and Planetary Change*, 36(3), 209-217, doi: 10.1016/S0921-8181(02)00186-8

744 Maiorano, P., Marino, M., Balestra, B., Flores, J.-A., Hodell, D.A., and Rodrigues, T., 2015.
745 Coccolithophore variability from the Shackleton Site (IODP Site U1385) through MIS 16-10.
746 *Global and Planetary Change*, 133, 35-48, <https://doi.org/10.1016/j.gloplacha.2015.07.009>.

747 Margari, V., Skinner, L.C., Hodell, D.A., Martrat, B., Toucanne, S., Grimalt, J.O., Gibbard,
748 P.L., Lunkka, J.P., and Tzedakis, P.C., 2014. Land-ocean changes on orbital and millennial time
749 scales and the penultimate glaciation. *Geology*, 42, 183-186.

750 Marino, M., Maiorano, P., Tarantino, F., Voelker, A., Capotondi, L., Girone, A., Lirer, F.,
751 Flores, J.-A., and Naafs, B. D. A., 2014. Coccolithophores as proxy of seawater changes at orbital-
752 to-millennial scale during middle Pleistocene Marine Isotope Stages 14–9 in North Atlantic core
753 MD01-2446. *Paleoceanography*, 29, 518-532, doi:10.1002/2013PA002574.

754 Marino, M., Girone, A., Maiorano, P., Di Renzo, R., Piscitelli, A., and Flores, J.A., 2018.
755 Calcareous plankton and the mid-Brunhes climate variability in the Alboran Sea (ODP Site 977).
756 *Palaeogeography, Palaeoclimatology, Palaeoecology*, 508, 91-106, doi:
757 10.1016/j.palaeo.2018.07.023.

758 Martrat, B., Grimalt J. O., Shackleton N., de Abreu L., Hutterli M. A., and Stocker T. F.,
759 2007. Four Climate Cycles of Recurring Deep and Surface Water Destabilizations on the Iberian
760 Margin. *Science*, 317, 502-507, doi: 10.1126/science.1139994.

761 McIntyre, A., and Bè, A. H. W., 1967. Modern coccolithophores of the Atlantic Ocean-I.
762 Placolith and cystoliths. *Deep-Sea Research and Oceanographic Abstracts*, 14(5), 561-597, doi:
763 10.1016/0011-7471(67)90065-4.

764 McManus, J., Oppo, D.W. and Cullen, J.L., 1999. A 0.5-million-year record of millennial-
765 scale climate variability in the North Atlantic. *Science*, 283, 971-975.

766 Milker, Y., Rachmayani, R., Weinkauf, M.F.G., Prange, M., Raitzsch, M., Schulz, M., and
767 Kučera, M., 2013. Global and regional sea surface temperature trends during Marine Isotope Stage
768 11. *Clim. Past* 9, 2231-2252.

769 Moita, M.T., Silva, A., Palma, S., and Vilarinho, M.G., 2010. The coccolithophore summer-
770 autumn assemblage in the upwelling waters of Portugal: Patterns of mesoscale distribution (1985-
771 2005). *Estuarine, Coastal and Shelf Science* 87, 411-419.

772 Molfino, B., and McIntyre, A. 1990. Nutricline variation in the equatorial Atlantic
773 coincident with the Younger Dryas. *Paleoceanography*, 5, 997-1008.

774 Morley, A., Rosenthal, Y., and de Menocal, P., 2014. Ocean-atmosphere climate shift during
775 the mid-to-late Holocene transition. *Earth and Planetary Science Letters*, 388, 18-26, doi:
776 10.1016/j.epsl.2013.11.039.

777 Okada, H., and McIntyre, A., 1979. Seasonal distribution of modern coccolithophores in the

778 western North Atlantic Ocean. *Marine Biology*, 54, 319-328.

779 Oliveira, D., Desprat, S., Rodrigues, T., Naughton, F., Hodell, D., Trigo, R., Rufino, M.,
780 Lopes, C., Abrantes, F., and Sánchez Goñi, M. F., 2016. The complexity of millennial-scale
781 variability in southwestern Europe during MIS 11. *Quaternary Research*, 86(3), 373-387, doi:
782 10.1016/j.yqres.2016.09.002.

783 Olsen, J., Anderson, N. J., and Knudsen, M. F., 2012. Variability of the North Atlantic
784 Oscillation over the past 5,200 years. *Nature Geoscience* 5, 808-812, doi:10.1038/ngeo1589.

785 Palumbo, E., Flores, J.A., Perugia, C., Emanuele, D., Petrillo, Z., Rodrigues, T., Voelker,
786 A.H.L., and Amore, F.O., 2013a. Abrupt variability of the last 24 ka recorded by coccolithophore
787 assemblages off the Iberian Margin (core MD03-2699). *Journal of Quaternary Science* 28(3), 320-
788 328.

789 Palumbo, E., Flores, J.A., Perugia, C., Petrillo, Z., Voelker, A.H.L., and Amore, F.O.,
790 2013b. Millennial scale Coccolithophore Paleoproductivity and surface water changes between 445
791 and 360 ka (Marine Isotope Stages 12/11) in the Northeast Atlantic. *Palaeogeography*
792 *Palaeoclimatology Palaeoecology*, 383-384, 27-41. doi:10.1016/j.palaeo.2013.04.024

793 Parente, A., Cachão, M., Baumann, K. H., de Abreu, L., and Ferreira, J., 2004.
794 Morphometry of *Coccolithus pelagicus* s: l. (Coccolithophore, Haptophyta) from offshore Portugal,
795 during the last 200kyr. *Micropaleontology*, 50 (1), 107-120, doi: 10.2113/50.Suppl_1.107.

796 Past Interglacial Working Group of PAGES, 2016. Interglacials of the last 800,000 years.
797 *Reviews of Geophysics*, 54, 162-219, doi:10.1002/2015RG000482.

798 Patterson, R.T. and Fishbein, E., 1989. Re-examination of the statistical methods used to
799 determine the number of point counts needed for micropaleontological quantitative research.
800 *Journal of Paleontology* 63, 245-248.

801 Peliz, A., Dubert, J., Santos, A.M.P., Oliveira, P.B. and Le Cann, B., 2005. Winter upper
802 ocean circulation in the Western Iberian Basin – fronts, eddies and poleward flows: an overview.
803 *Deep Sea Research Part I: Oceanographic Research Papers* 52, 621-646.

804 Pérez, F.F., Castro, C.G., Alvarez-Salgado, X.A., and Rios, A. F., 2001. Coupling between
805 the Iberian basin – scale circulation and the Portugal boundary current system: a chemical study.
806 *Deep Sea Research Part I: Oceanographic Research Papers* 48, 1519-1533.

807 Pol, K., Masson-Delmotte, V., Johnsen, S., Bigler, M., Cattani, O., Durand, G., Falourd, S.,
808 Jouzel, J., Minster, B., Parrenin, F., Ritz, C., Steen-Larsen, H.C., and Stenni, B., 2010. New MIS 19
809 EPICA Dome C high resolution deuterium data: Hints for a problematic preservation of climate
810 variability at sub-millennial scale in the “oldest ice”. *Earth and Planetary Science Letters*, 298(1-2),
811 95-103, doi: 10.1016/j.epsl.2010.07.030.

812 Poulton, A.J., Holligan, P.M., Charalampopoulou, A., and Adey, T.R., 2017.
813 Coccolithophore ecology in the tropical and subtropical Atlantic Ocean: New perspectives from the
814 Atlantic meridional transect (AMT) programme. *Progress in Oceanography* 158, 150-170.

815 Regattieri, E., Giaccio, B., Galli, P., Nomade, S., Peronace, E., Messina, P., Sposato, A.,
816 Boschi, C., and Gemelli, M., 2016. A multi-proxy record of MIS 11–12 deglaciation and glacial
817 MIS 12 instability from the Sulmona basin (central Italy). *Quaternary Science Reviews*, 132, 129-
818 145, doi: 10.1016/j.quascirev.2015.11.015.

819 Relvas, P., Barton, E.D., Dubert, J., et al. 2007. Physical oceanography of the western Iberia
820 ecosystem: latest views and challenges. *Progress in Oceanography* 74, 149-173.

821 Repschläger, J., Garbe-Schönberg, D., Weinelt, M., and Schneider, R., 2017. Holocene
822 evolution of the North Atlantic subsurface transport. *Clim. Past*, 13, 333-344, doi:10.5194/cp-13-
823 333-2017.

824 Reyes, A.V., Carlson, A.E., Beard, B.L., Hatfield, R.G., Stoner, J.S., Winsor, K., Welke, B.,
825 and Ullman, D.J., 2014. South Greenland ice-sheet collapse during Marine Isotope Stage 11. *Nature*
826 510, 525-528.

827 Rios, A., Pérez, F., and Fraga, F., 1992. Water masses in the upper and middle North
828 Atlantic Ocean east of the Azores. *Deep-Sea Research Part A. Oceanographic Research Papers*, 39
829 (3-4), 645-658, doi: 10.1016/0198-0149(92)90093-9.

830 Rodrigues T., Grimalt J. O., Abrantes F., Naughton F., and Flores J. A., 2010. The last
831 glacial-interglacial transition (LGIT) in the western mid-latitudes of the North Atlantic: Abrupt sea
832 surface temperature change and sea level implications. *Quaternary Science Reviews* 29(15-16):
833 1853-1862.

834 Rodrigues, T., Alonso-García, M., Hodell, D.A., Rufino, M., Naughton, F., Grimalt, J.O.,
835 Voelker, A.H.L., and Abrantes, F., 2017. A 1-Ma record of sea surface temperature and extreme
836 cooling events in the North Atlantic: A perspective from the Iberian Margin. *Quaternary Science*
837 *Reviews* 172, 118-130.

838 Rodrigues, T., Voelker, A. H. L., Grimalt, J. O., Abrantes, F., Naughton, F., 2011. Iberian
839 Margin sea surface temperature during MIS 15 to 9 (580–300 ka): Glacial suborbital variability
840 versus interglacial stability. *Paleoceanography*, 26, PA1204, doi:10.1029/2010PA001927.

841 Rohling, E.J., Braun, K., Grant, K., Kucera, M., Roberts, A.P., Siddall, M., and Trommer,
842 G., 2010. Comparison between Holocene and Marine Isotope Stage-11 sea-level histories. *Earth and*
843 *Planetary Science Letters*, 291(1-4), 97-105, doi: 10.1016/j.epsl.2009.12.054.

844 Roth, P.H., 1994. Distribution of coccoliths in oceanic sediments. In: Winter, A., Siesser,
845 W.G. (Eds.), *Coccolithophores*. Cambridge, University Press, Cambridge, pp. 199-218.

846 Ruddiman, W.F., 2003. Orbital insolation, ice volume, and greenhouse gases. *Quaternary*
847 *Science Reviews* 22, 1597-1629.

848 Saavedra-Pellitero, M., J. A. Flores, F. Lamy, F. J. Sierro, and A. Cortina, 2011.
849 Coccolithophore estimates of paleotemperature and paleoproductivity changes in the southeast
850 Pacific over the past ~27 kyr. *Paleoceanography*, 26, PA1201, doi:10.1029/2009PA001824.

851 Saavedra-Pellitero, M., Baumann, K.-H., Ullermann, J. and Lamy, F., 2017. Marine Isotope
852 Stage 11 in the Pacific sector of the Southern Ocean; a coccolithophore perspective. *Quaternary*
853 *Science Reviews*, 158, 1-14, doi: 10.1016/j.quascirev.2016.12.020.

854 Salgueiro E., Voelker A.H.L., de Abreu L., et al. 2010. Temperature and productivity
855 changes off the western Iberian margin during the last 150 ky. *Quaternary Science Reviews* 29:
856 680-695.

857 Salgueiro, E., Naughton, F., Voelker, A.H.L., de Abreu, L., Alberto, A., Rossignol, L.,
858 Duprat, J., Magalhães, V.H., Vaqueiro, S., Turon, J.-L., and Abrantes, F., 2014. Past circulation
859 along the western Iberian margin: a time slice vision from the Last Glacial to the Holocene.
860 *Quaternary Science Reviews*, 106, 316-329, doi: 10.1016/j.quascirev.2014.09.001.

861 Sánchez R. F., Relvas P., and Delgado M., 2007. Coupled ocean wind and sea surface
862 temperature patterns off the western Iberian Peninsula. *Journal of Marine Systems* 68, 103-127.

863 Sánchez-Goñi, M.F., Llave, E., Oliveira, D., Naughton, F., Desprat, S., Ducassou, E.,
864 Hodell, D. A., and Hernández-Molina, F.J., 2016. Climate changes in south western Iberia and
865 Mediterranean Outflow variations during two contrasting cycles of the last 1Myrs: MIS 31–MIS 30
866 and MIS 12–MIS 11. *Global and Planetary Change*, 136, 18-29, doi:
867 10.1016/j.gloplacha.2015.11.006.

868 Schulz, M., and Mudelsee, M., 2002. REDFIT: estimating spectra directly from unevenly
869 spaced paleoclimatic time series. *Computer & Geosciences*, 28 (3), 421-426, doi: 10.1016/S0098-
870 3004(01)00044-9.

871 Schwab, C., Kinkel, H., Weinelt, M. and Repschlaeger, J., 2012. Coccolithophore
872 paleoproductivity and ecology response to deglacial and Holocene changes in the Azores Current
873 System. *Paleoceanography* 27(3), PA3210, doi: 10.1029/2012pa002281.

874 Shackleton, N.J., Hall, M.A. and Vincent, E., 2000. Phase relationships between millennial-
875 scale events 64,000 – 24,000 years ago, *Paleoceanography* 15 (6), 565- 569, doi:
876 10.1029/2000PA000513.

877 Skinner, L.C., Shackleton, N.J., and Elderfield, H., 2003. Millennial-scale variability of
878 deep-water temperature and $\delta^{18}\text{O}_{\text{dw}}$ indicating deep-water source variations in the Northeast

879 Atlantic, 0-34 cal. ka BP. *Geochemistry Geophysics Geosystems* 4(12), 1098, doi:
880 10.1029/2003GC000585.

881 Stepanchuk, V. N., and Moigne, A.-M., 2016. MIS 11-locality of Medzhibozh, Ukraine:
882 Archaeological and paleozoological evidence. *Quaternary International*, 409 (Part B), 241-254, doi:
883 10.1016/j.quaint.2015.09.050.

884 Thomson, D. J., 1990. Time series analysis of Holocene climate data. *Philosophical*
885 *Transactions of the Royal Society of London. Series A* 330, 601-616.

886 Trigo R.M., Pozo-Vazquez D., Osborn T. J., et al. 2004. North Atlantic oscillation influence
887 on precipitation, river flow and water resources in the Iberian Peninsula. *International Journal of*
888 *Climatology* 24, 925-944.

889 Tzedakis P. C., 2010. The MIS 11 – MIS 1 analogy, southern European vegetation,
890 atmospheric methane and the "early anthropogenic hypothesis". *Climate of the Past*, 6, 131-144,
891 doi: 10.5194/cp-6-131-2010.

892 Tzedakis P. C., Channell J. E. T., Hodell D. A., Kleiven H. F., and Skinner L. C., 2012.
893 Determining the natural length of the current interglacial. *Nature Geoscience*, 5(2), 138-141, doi:
894 10.1038/ngeo1358.

895 Vázquez Riveiros, N., Waelbroeck, C., Skinner, L., Duplessy, J. C., McManus, J. F.,
896 Kandiano, E. S., and Bauch, H. A., 2013. The "MIS 11 paradox" and ocean circulation: Role of
897 millennial scale events. *Earth and Planetary Science Letters*, 371-372, 258-268, doi:
898 10.1016/j.epsl.2013.03.036.

899 Voelker, A. H. L., Rodrigues, T., Billups, K., Oppo, D. W., McManus, J. F., Stein, R.,
900 Hefter, J., and Grimalt, J. O., 2010. Variations in mid-latitude North Atlantic surface water
901 properties during the mid-Brunhes (MIS 9–14) and their implications for the thermohaline
902 circulation. *Climate of the Past* 6, 531-552, doi:10.5194/cp-6-531-2010.

903 Wanner, H. Beer, J., Bütikofer, J., Crowley, T. J., Cubasch, U., Flückiger, J., Goosse, H.,
904 Grosjean, M., Joos, F., Kaplan, J. O., Küttel, M., Müller, S. A., Prentice, I. C., Solomina, O.,
905 Stocker, T. F., Tarasov, P., Wagner, M., and Widmann, M., 2008. Mid- to Late Holocene climate
906 change: an overview. *Quaternary Science Reviews*, 27 (19-20), 1791-1828, doi:
907 10.1016/j.quascirev.2008.06.013.

908 Wassenburg, J. A., Dietrich, S., Fietzke, J., Fohlmeister, J., Jochum, K. P., Scholz, D.,
909 Richter, D.K., Sabaoui, A., Spötl, C., Lohmann, G., Andreae, M. O., and Immenhauser, A., 2016.
910 Reorganization of the North Atlantic Oscillation during early Holocene deglaciation. *Nature*
911 *Geoscience*, 9, 602-, <http://dx.doi.org/10.1038/ngeo2767>.

912 Weirauch, D., Billups, K., and Martin, P., 2008. Evolution of millennial-scale climate
913 variability during the mid-Pleistocene. *Paleoceanography*, 23, PA3216,
914 doi:10.1029/2007PA001584.

915 Winter, A., Jordan, R.W., Roth, P.H., 1994. Biogeography of living Coccolithophores
916 in ocean waters. In: Winter, A., Siesser, W.G. (Eds.), *Coccolithophores*. Cambridge
917 University Press, Cambridge, pp. 199-218.

918 Yin Q. Z., and Berger A., 2010. Insolation and CO₂ contribution to the interglacial climate
919 before and after the Mid-Brunhes Event. *Nature Geoscience*, 3(4), 243-246.
920 <http://dx.doi.org/10.1038/ngeo771>.

921 Zeeden, C., Hilgen, F., Westerhold, T., Lourens, L., Röhl, U., and Bickert, T., 2016. Revised
922 Miocene splice, astronomical tuning and calcareous plankton biochronology of ODP Site 926
923 between 5 and 14.4 Ma. *Palaeogeography, Palaeoclimatology, Palaeoecology*, 369, 430-451,
924 <https://doi.org/10.1016/j.palaeo.2012.11.009>.

925
926

927 **Figure captions**

928 **Figure 1.** Core location and modern surface oceanographic and atmospheric setting off western
929 Iberia for Spring-Summer (A) and Autumn-Winter (B) (modified from Palumbo et al., 2013b). IL =
930 Icelandic Low; AH = Azores High; NAC = North Atlantic Current; AzC = Azores Current; IPC =
931 Iberian Poleward Current; ENACWst= Eastern North Atlantic Central Waters of subtropical origin;
932 ENACWsp= Eastern North Atlantic Central Waters of subpolar origin.

933

934 **Figure 2.** Deglaciation and precession cycle alignments of the last 24 ka BP and 445-360 ka
935 intervals. In the top panel, the black line shows the SST (°C) data for 445-360 ka (Rodrigues et al.,
936 2011) and the colored lines the SST record for the last 24 ka BP (Rodrigues et al., 2010) according
937 to the deglaciation (magenta) and precession (red) alignments. Stippled lines in the bottom panel
938 indicate the precession amplitude (Berger and Loutre, 1991) for the interval 445-360 ka (black) and
939 the last 24 ka BP (red), respectively.

940

941 **Figure 3.** Comparison of coccolithophore assemblage and alkenone data for MIS 1 vs. MIS 11.
942 From bottom to the top in each panel: paleoproductivity proxy (i.e., total nannofossil accumulation
943 rate for MIS 1 and small *Gephyrocapsa* accumulation rate for MIS 11); subpolar surface waters
944 proxies (% *C. pelagicus* ssp. *pelagicus* and %C_{37:4}). Colored vertical bars represent periods of major
945 specific surface-ocean current persistence: yellow for Portugal Current (PC); cyan for subpolar
946 surface waters (SPWs); green for surface-ocean instability; pink for Iberian Poleward Current (IPC)

947 transporting ENACWst. Stratigraphic abbreviations are: Ht 4 for Heinrich-type event 4; T (as in
948 TV, T1a) for Termination; YD for Younger Dryas; B/A for Bølling-Allerød; H1 for Heinrich event
949 1; LGM for last glacial maximum; GS for Greenland stadial; and GI for Greenland interstadial.

950

951 **Figure 4.** Additional coccolithophore assemblage data for MIS 1 vs. MIS 11. From bottom to the
952 top in each panel: Iberian Poleward Current (IPC) proxy (% *U. sibogae*); Azores Current (AzC)
953 proxy (% *C. pelagicus* ssp. *azorinus*); surface water oligotrophy proxy (% *F. profunda*). Colored
954 vertical bars and stratigraphic abbreviations are the same as in Figure 3.

955

956 **Figure 5.** PCA performed on 445-360 ka and last 24 ka BP intervals. Upper panel: scatter diagrams
957 for the last 24 ka BP between (A) components 1 and 2 and (B) components 1 and 3. Lower panel:
958 scatter diagrams for 445-360 ka interval between (C) components 2 and 1 and (D) components 3
959 and 1. Tables on the left side provide specification of components used in the analyses (central
960 panel), eigenvalues and percentages of variance for each component with upper table referring to
961 the last 24 ka BP and lower table to the 445-360 ka interval.

962

963 **Figure 6.** PCA performed for deglaciation period for MIS 2-MIS 1 (19-13.5 ka BP) and MIS 12 –
964 MIS 11 (430-425 ka). (A) scatter diagram between components 2 and 1 for MIS 2-MIS 1
965 deglaciation; (B) scatter diagram between components 3 and 1 for MIS 12-MIS 11 deglaciation.
966 Tables on the left side as in Figure 5.

967

968 **Figure 7.** PCA performed on early-to-mid Holocene (12-7 ka BP) and MIS11c (409-402 ka). (A)
969 scatter diagram between components 3 and 1 for the early-to-mid Holocene; (B) scatter diagram
970 between components 2 and 1 for MIS11c. Tables on the left side as in Figure 5.

971

972 **Figure 8.** Periodograms of investigated taxa obtained using REDFIT for the last 24 ka BP interval.
973 In the periodograms, dotted red lines indicate red noise (Theor AR(1)), green and yellow dotted
974 lines represent 90% and 95% significance levels, respectively. Bottom x-axis refers to frequency
975 scale, top x-axis to periodicity scale. Green vertical bars represent the Bandwidth. Numbers on
976 periodograms indicate precession periodicities.

977

978 **Figure 9.** Periodograms of investigated taxa obtained using REDFIT for the 445-360 ka interval. In
979 the periodograms, dotted red lines indicate red noise (Theor AR(1)), green and yellow dotted lines
980 represent 90% and 95% significance levels, respectively. Bottom x-axis refers to frequency scale,

981 top x-axis to periodicity scale. Green vertical bars represent the Bandwidth. Numbers on
 982 periodograms indicate precession periodicities.

983

984 **Table 1**

Coccolithophore assemblages	Ecological preferences with main references	Alkenone data	Surface Ocean Conditions off Iberian Margin
<i>U. sibogae</i>	warm and oligotrophic surface waters (McIntyre and Bè, 1967; Brand, 1994; Roth, 1994; López-Otálvaro et al., 2009; Amore et al., 2012; Palumbo et al., 2013a, b)	increased alkenones-derived SST	Iberian Poleward Current
<i>C. pelagicus</i> ssp. <i>pelagicus</i>	cold surface waters related to subpolar front (Parente et al., 2004)	decreased alkenones-derived SST	subpolar surface waters
small <i>Gephyrocapsa</i> accumulation rate (MIS 11); Total Nannofossil Accumulation Rate (MIS1)	nutrient-rich surface waters (Baumann et al., 2004; López-Otálvaro et al., 2009; Saavedra-Pellitero et al., 2011; Amore et al., 2012; Palumbo et al., 2013a, b)	not-relevant	Portugal Current
<i>C. pelagicus</i> ssp. <i>azorinus</i>	warm surface waters transported by Azores Current (Parente et al., 2004)	increased alkenones-derived SST	Azores Current
Sum of cold species (<i>C. pelagicus pelagicus</i> ; <i>Gephyrocapsa muellerae/margereli</i> ; <i>Emiliana huxleyi</i> >4µm)	cold and nutrient-poor surface waters (McIntyre and Bè, 1967; Breheret, 1978; Roth, 1994; Flores et al., 1997; Flores et al., 2010; Amore et al., 2012; Palumbo et al., 2013a, b)	increased C _{37:4} % decreased alkenones-derived SST	waters with melting icebergs cold surface waters

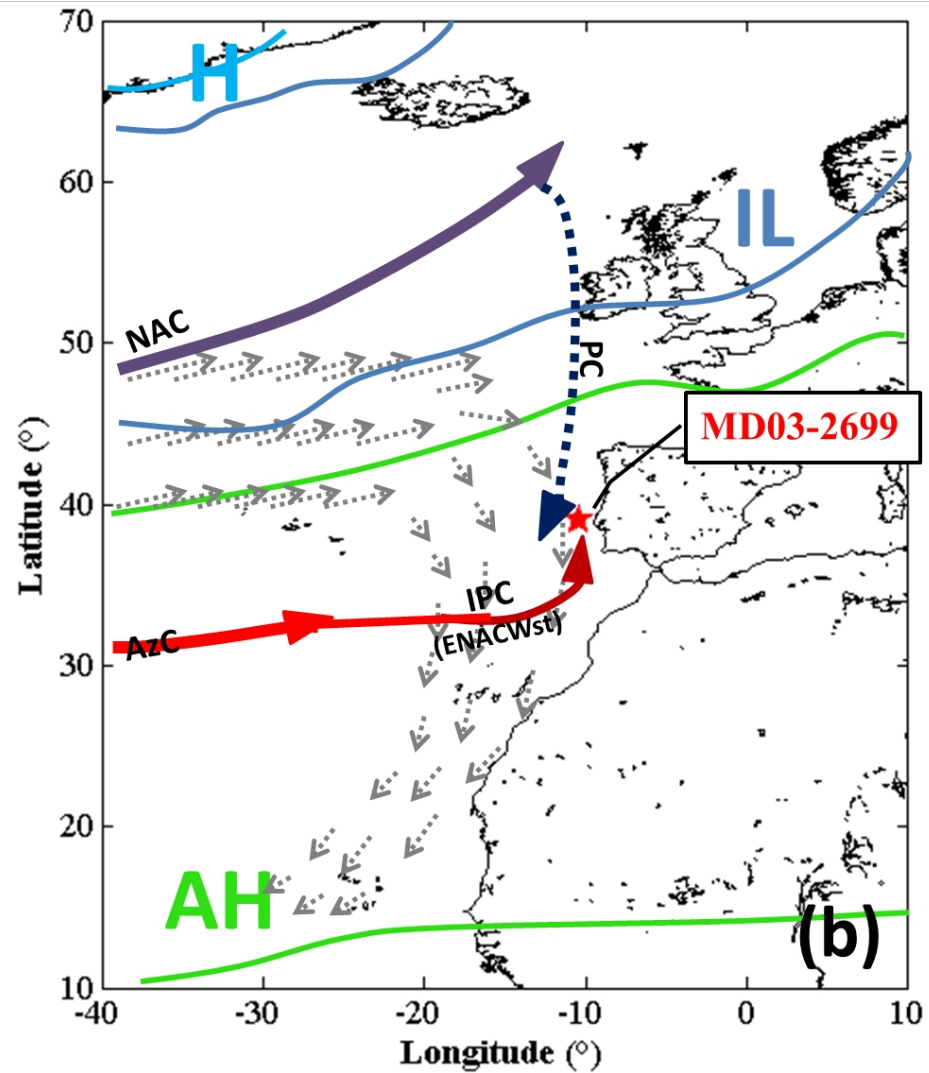
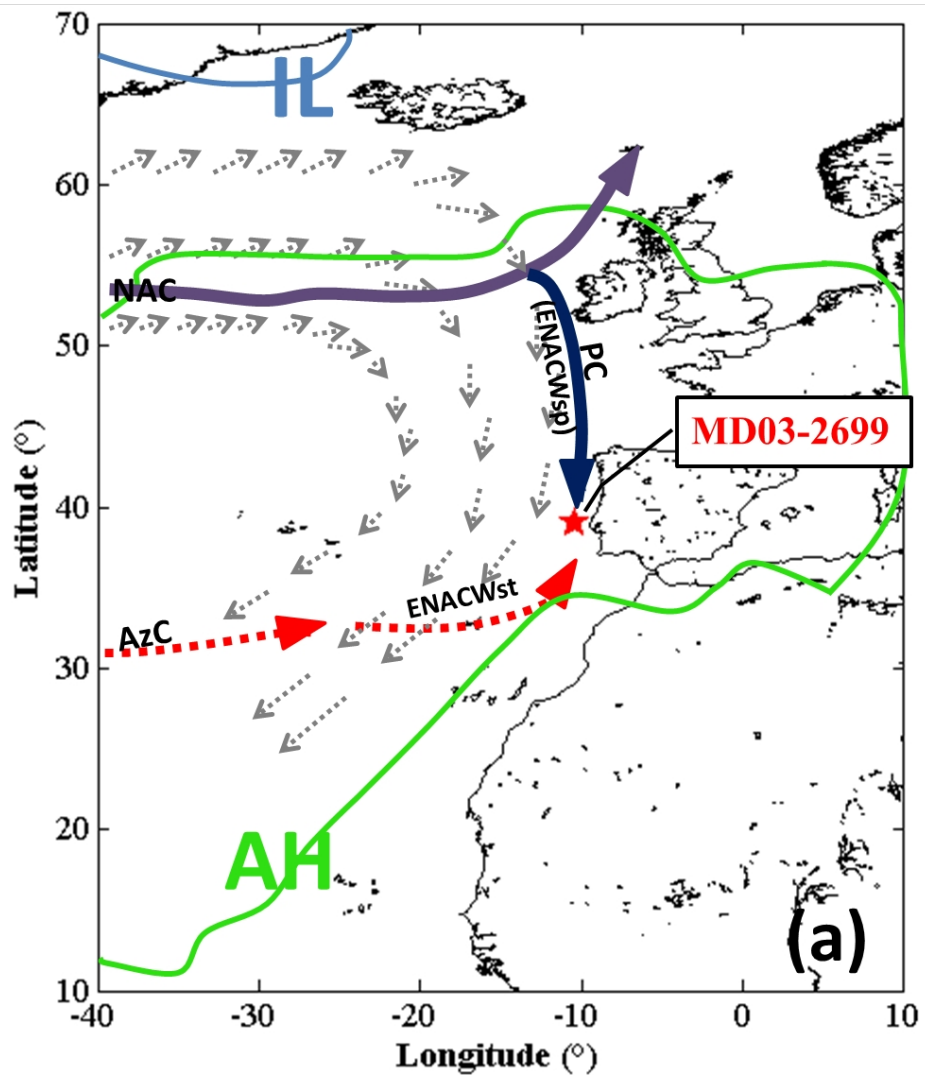
985 Remarks: Coccolithophore assemblages and their main ecological preferences combined with alkenone data
 986 characterising the main surface ocean currents off Iberian Margin. Original descriptions are reported in
 987 Rodrigues et al. (2011), Amore et al. (2012) and Palumbo et al. (2013a, b).

988

989

990

991



Age (ka BP)

0 2 4 6 8 10 12 14 16 18 20 22 24

— deglaciations alignment
— precession alignment

Age (ka BP)

0 2 4 6 8 10 12 14 16 18 20 22 24

20
19
18
17
16
15
14
13
12
11
10
9
8
7
6
MD03-2699 SST (°C)

Ht 4

Age (ka)

360 365 370 375 380 385 390 395 400 405 410 415 420 425 430 435 440 445

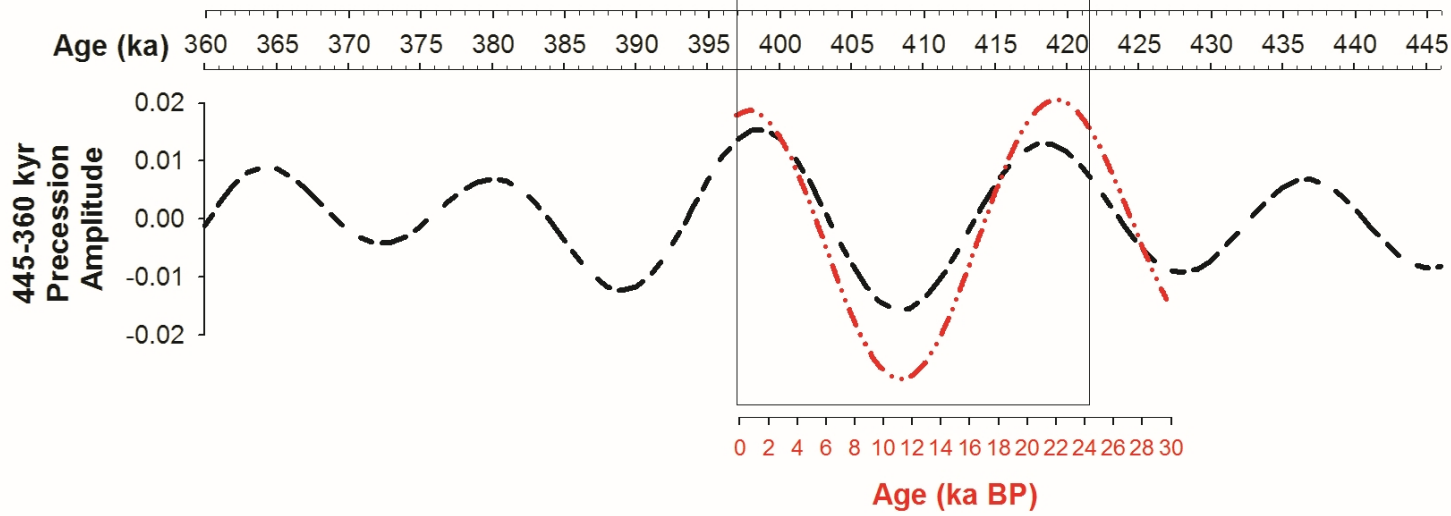
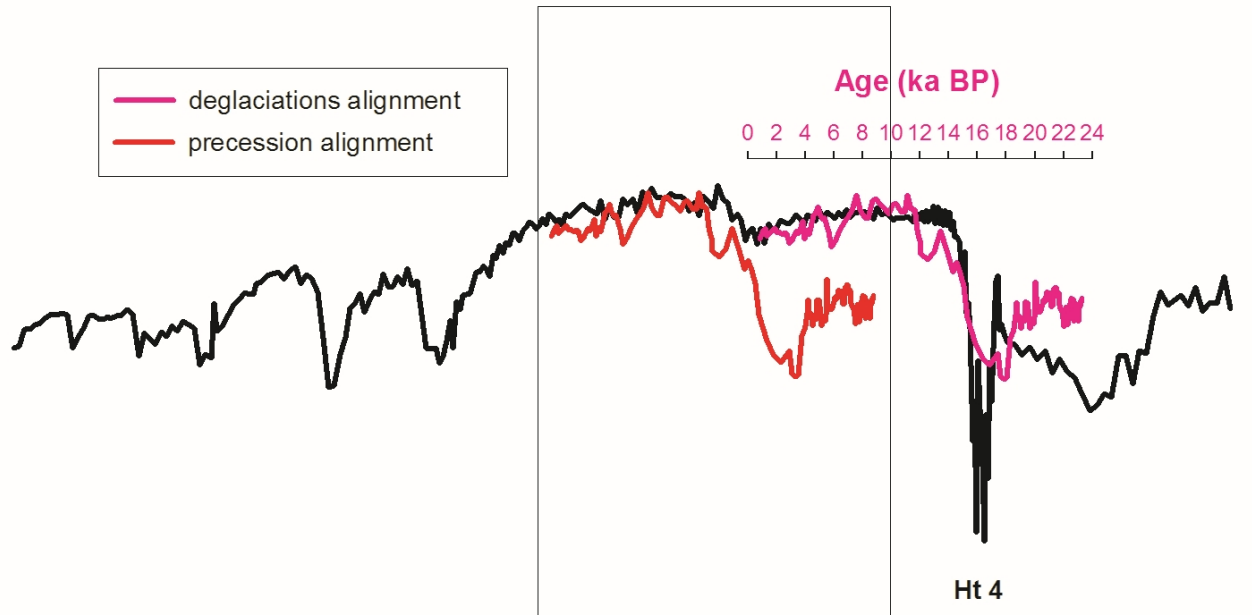
445-360 kyr
Precession
Amplitude

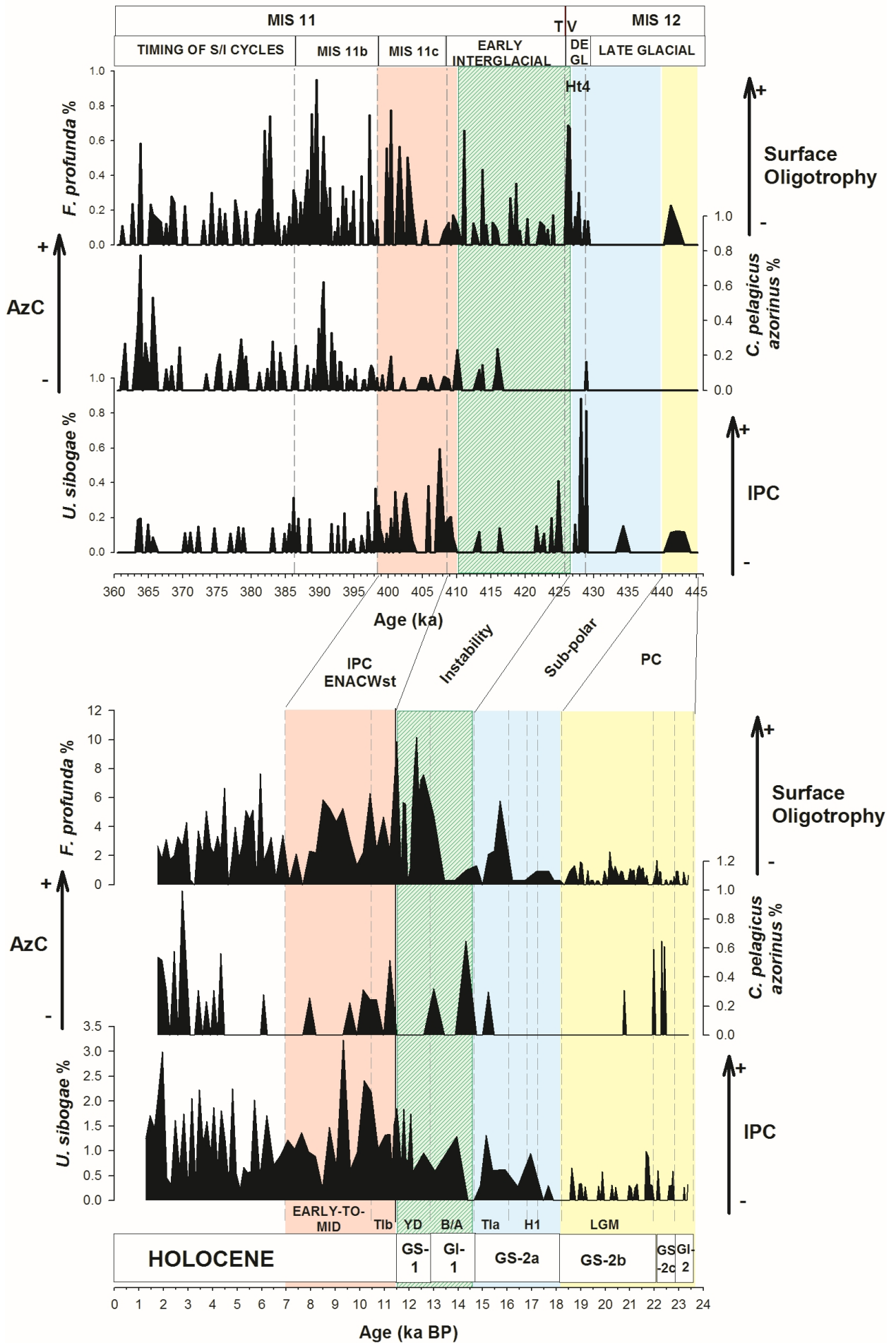
0.02
0.01
0.00
-0.01
-0.02

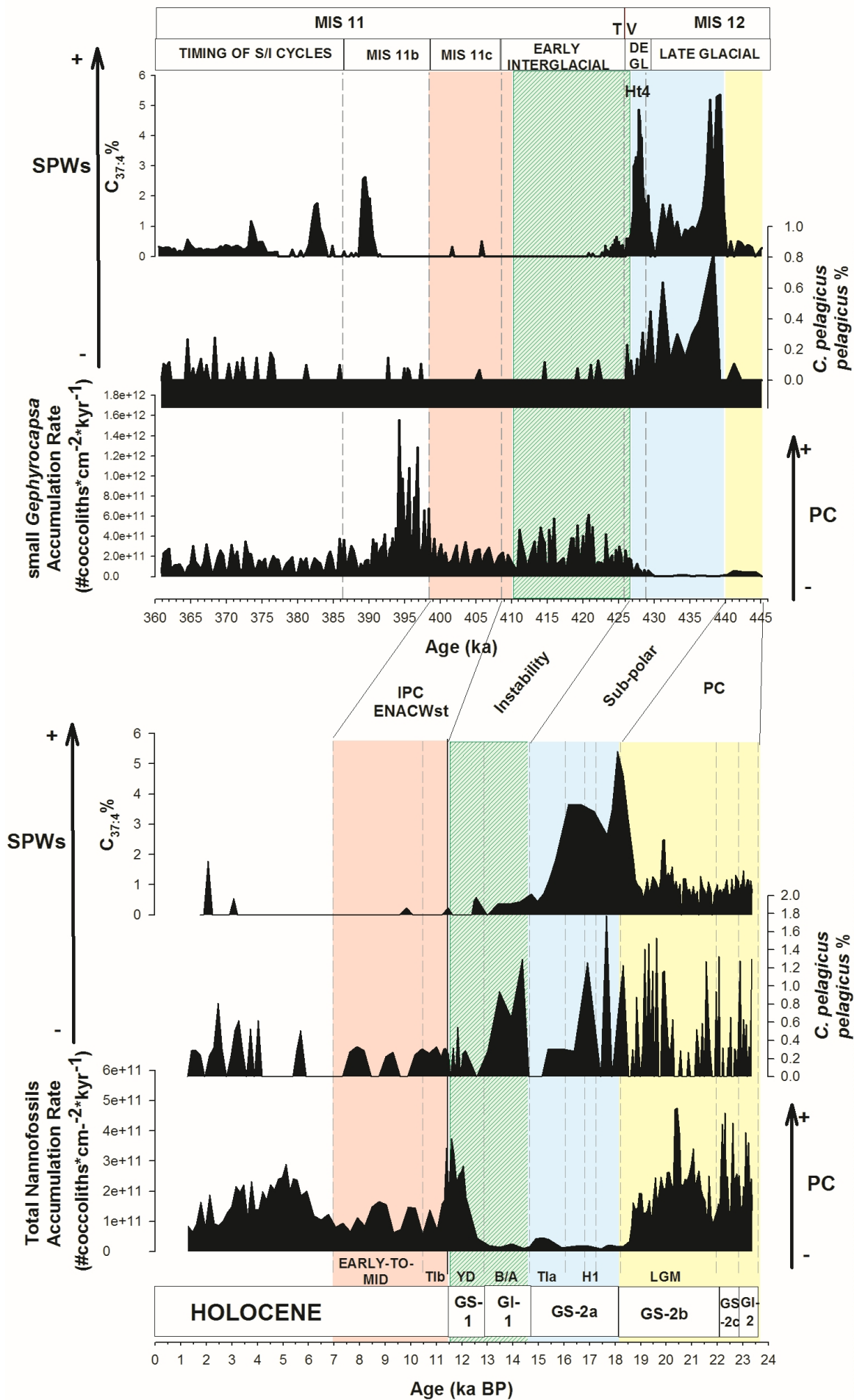
0.03
0.02
0.01
0.00
-0.01
-0.02
-0.03
last 24 kyr
Precession Amplitude

0 2 4 6 8 10 12 14 16 18 20 22 24 26 28 30

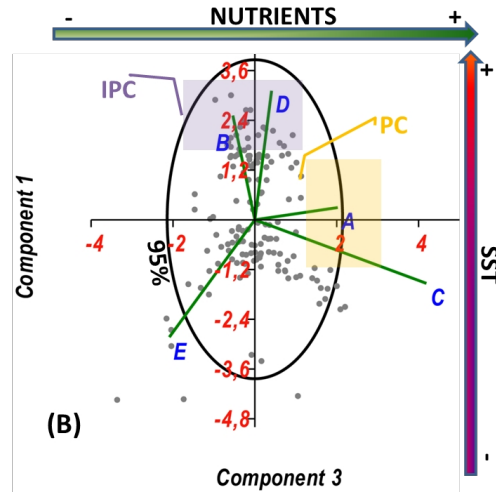
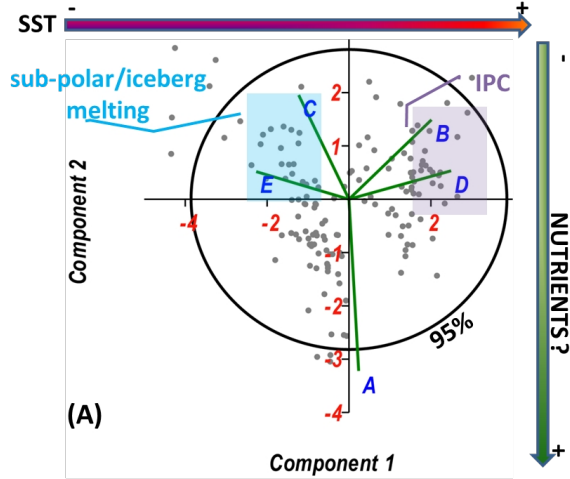
Age (ka BP)







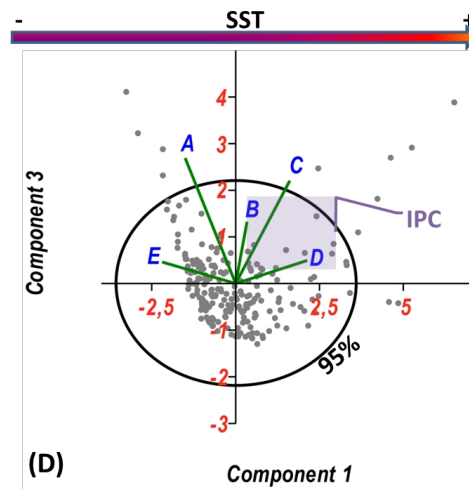
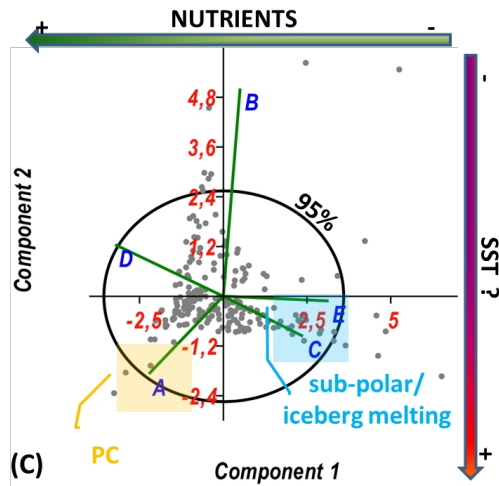
MIS 1 FULL TREND



Components	Eigenvalue	% Variance
1	2.4	47.9
2	1.3	25.6
3	0.7	14.8

A	NAR(*) ; small <i>Gephyrocapsa</i> NAR(**)
B	<i>U. sibogae</i> %
C	<i>C. pelagicus ssp. pelagicus</i> %
D	SST
E	C _{37:4} %

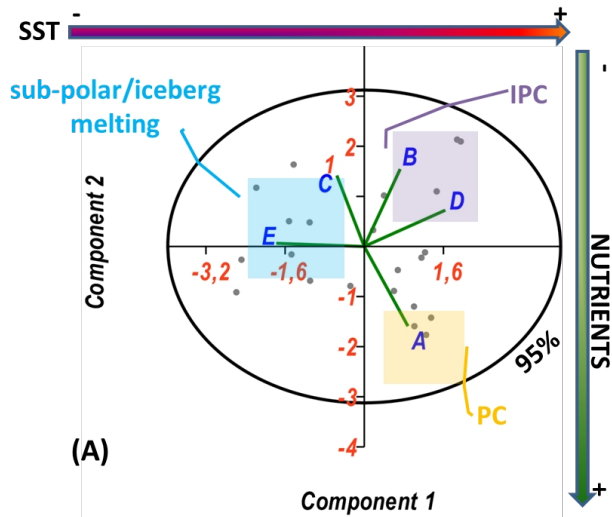
MIS 11 FULL TREND



Components	Eigenvalue	% Variance
1	2.17	41.9
2	1.1	21.3
3	0.8	15.7

PC = Portugal Current
IPC = Iberian Poleward Current

**19-13.5 ka BP (MIS 1 – MIS 2
Deglaciation)**

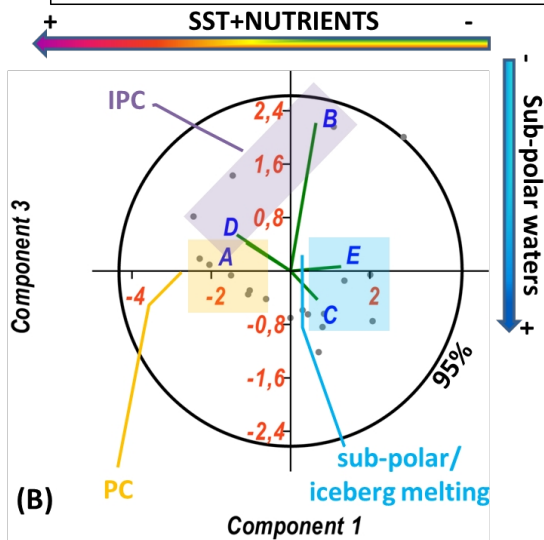


Components	Eigenvalue	% Variance
------------	------------	------------

1	2.2	43.2
2	1.4	26.7

A	NAR ^(*) ; small <i>Gephyrocapsa</i> NAR ^(**)
B	<i>U. sibogae</i> %
C	<i>C. pelagicus</i> ssp. <i>pelagicus</i> %
D	SST
E	C _{37:4} %

**430-425 ka (MIS 11 – MIS 12
Deglaciation)**

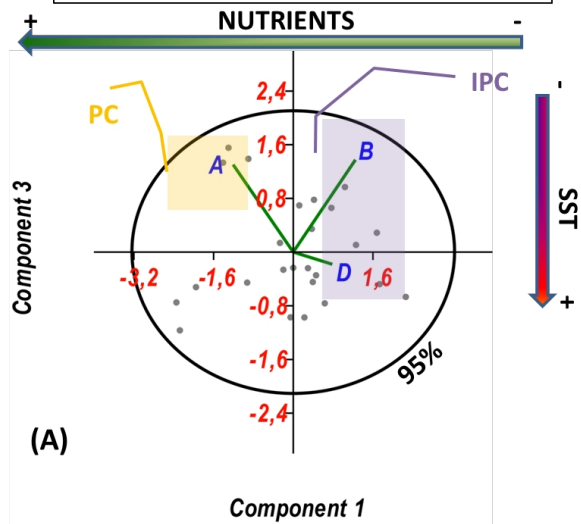


Components	Eigenvalue	% Variance
------------	------------	------------

1	2.5	48.9
2	0.9	19.8

PC = Portugal Current
IPC = Iberian Poleward Current

12 – 7 ka BP (early-to-mid Holocene)

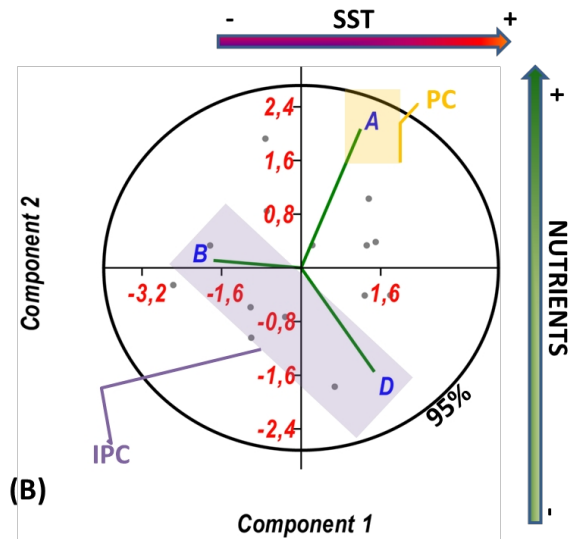


Components	Eigenvalue	% Variance
------------	------------	------------

1	1.5	49.1
2	0.9	30.2

A	NAR ^(*) ; small <i>Gephyrocapsa</i> NAR ^(**)
B	<i>U. sibogae</i> %
D	SST

409- 402 ka BP (MIS 11c)



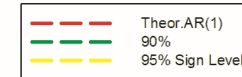
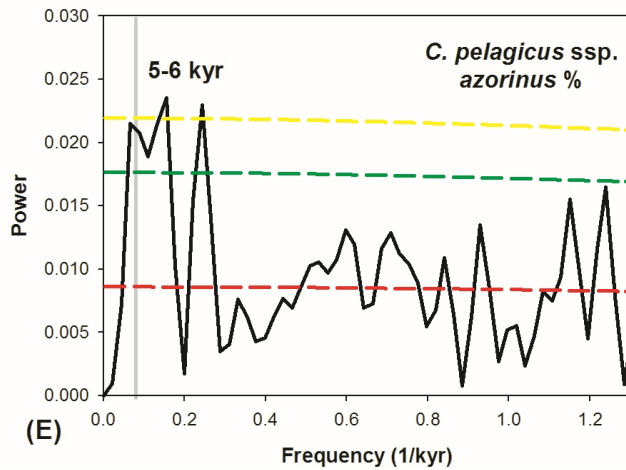
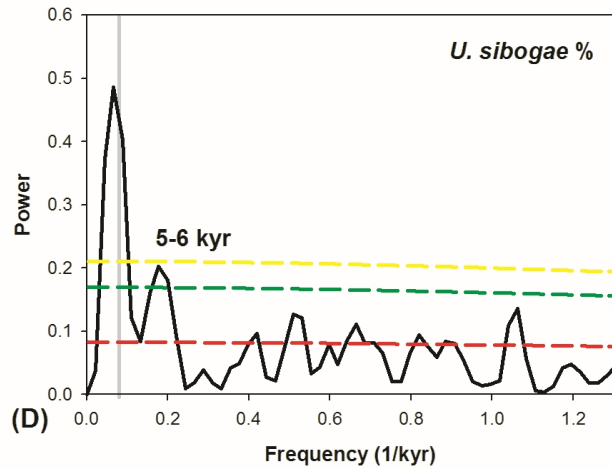
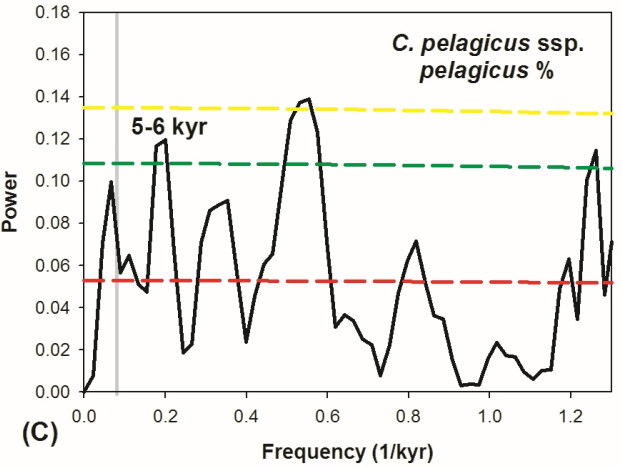
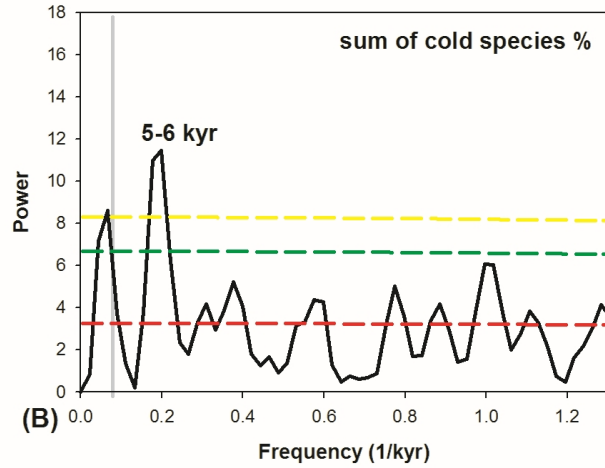
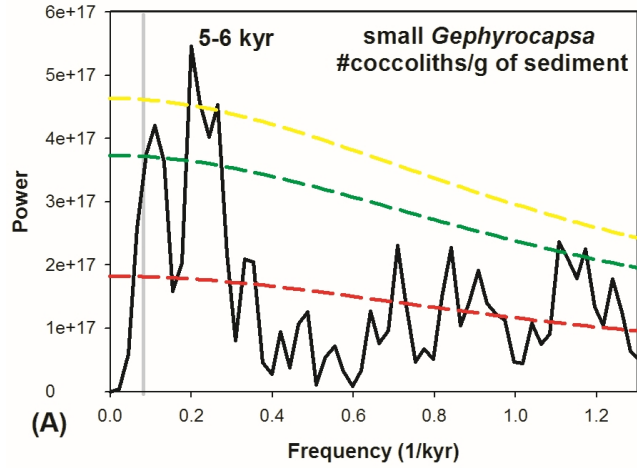
Components	Eigenvalue	% Variance
------------	------------	------------

1	1.9	62.3
2	0.9	29.4

PC = Portugal Current

IPC = Iberian Poleward Current

MIS 1 - MIS 2 (0.75-24 ka BP)



MIS 11 - MIS 12 (360-445 ka)

